Epigenetic regulation of tumor progression and metastasis by chromatin remodeling factor SATB1

Jong-Joo Lee

Department of Medical Science
The Graduate School, Yonsei University

Epigenetic regulation of tumor progression and metastasis by chromatin remodeling factor SATB1

Directed by Professor Hyoung-Pyo Kim

The Doctoral Dissertation
submitted to the Department of Medical Science,
the Graduate School of Yonsei University
in partial fulfillment of the requirements for the degree of
Doctor of Philosophy

Jong-Joo Lee

June 2016

This certifies that the Doctoral Dissertation of Jong-Joo Lee is approved.

_____

Thesis Supervisor: Hyoung-Pyo Kim

_____

Thesis Committee Member #1: Ho-Geun Yoon

_____

Thesis Committee Member #2: Kyung-Hee Chun

_____

Thesis Committee Member #3: Yoonsoo Hahn

_____

Thesis Committee Member #4: Kyoung Yul Seo

The Graduate School
Yonsei University

June 2016

ACKNOWLEDGEMENTS

학위과정을 마치는 이 시점에 여러 생각들이 주마등처럼 스쳐 지나갑니다. 학위과정을 하는 동안 정말 크고 작은 많은 일들이 있었습니다. 수많은 어려움 속에서 여러 분들께서 저에게 보이는 곳에서 또는 보이지 않는 곳에서 항상 응원해 주시고 도움을 주셨기에 이렇게 잘 마무리 할 수 있다고 생각합니다.

먼저, 아무것도 할 줄 아는 것도 없었던 저에게 이렇게 큰 일을 이룰 수 있게 깊은 애정과 따뜻한 지도로 이끌어 주신 저의 지도교수님 김형표 교수님께 가장 큰 감사와 존경을 표합니다. 교수님 덕분에 이렇게 학위과정을 무사히 마칠 수 있었습니다. 바쁘신 와중에도 학위 논문이 완성되기까지 아낌없이 조언 해주시고, 심사 해주신 심사위원 교수님들, 윤호근 교수님, 전경희 교수님, 서경률 교수님, 그리고 중앙대학교 한윤수 교수님께도 깊이 감사 드립니다.

학위과정을 하면서 어렵고 힘들일 있을 때마다 큰 도움을 준 또 하나의 저의 가족이었던 우리 실험실 사람들에게도 감사의 인사를 이 글을 통해서 전합니다. 학위 논문을 완성을 하는데 가장 큰 도움을 준 미경이, 고민이나 위기가 있을 때마다 많은 조언 해 준 민지, 실험실 선배로서 많이 부족했지만, 항상 따라주고 도움 줬던 예은이, 수언이. 진심으로 고맙습니다. 또한 실험을 진행하면서 조언과 격려를 아끼지 않은 태균이, 남영희 선생님, 지금은 안 계시지만, 많은 실험을 가르쳐 주신 주경돈 박사님, 박주홍 박사님, 정연욱 박사님, 박근희 선생님 감사합니다. 서로 다른 주제로 연구하고 있지만, 학위과정에 많은 도움을 주신 미생물학교실 이현규 선생님 이 자리를 빌어서 진심으로 감사 드립니다. 아울러 환경의생물학교실 용태순 교수님, 박순정 교수님, 신명헌 교수님, 그리고 여러 교실 선생님들 감사합니다.

친구라는 이름만으로도 큰 힘이 되었던 욱진이, 주호, 영수. 너희가 있어서 고비 때마다 유쾌하게 넘길 수 있었다. 정말 고마워. 대학원 생활을 하면서 물심양면으로 많은 도움을 준 윤희형, 정호, 철환이, 연희, 그리고 많은 디스커션을 나눴던 원석이, 한나, 나라, 창훈이 에게도 감사의 말 전합니다. 자주 만나지 못하지만 항상 응원해주고 아낌 없이 격려해 준 고등학교 친구,

김대현, 김경섭, 안대현, 이용재, 이재현, 정지화, 군대에서 동고동락했던 용만이형, 일문이형, 일형이형, 원상이, 민제에게도 감사의 말을 전합니다.

마지막으로, 학위를 진행하면서 제 뜻을 존중하고 믿어 주시며 뒷바라지 하느라 고생하신, 사랑하는 우리 아버지, 어머니께 마음 속 깊이 감사하고 사랑합니다. 항상 한결같이 응원으로 큰 힘이 되어주신 아버님과 어머님께도 진심으로 감사 드립니다. 멀리 떨어져 있지만 오빠를 위해 많이 기도하고 응원해주는 동생 이현주, 매제 이경준, 그리고 조카들, 많이 챙겨주지 못해서 항상 미안한 처남에게도 고맙다는 말 전합니다. 그리고 넘어져서 좌절하고 힘들 때 옆에서 항상 응원해주고, 격려해주고, 가장 내 편이 되어준 사랑하는 아내 곽아름에게도 무한한 감사의 말을 전합니다.

모두 언급하지는 못했지만, 그 외 정말 많은 분들의 도움이 있었기에 학위과정을 마무리 할 수 있었습니다. 박사를 마무리하는 이 시점에서도 아직 부족한 게 더 많다고 생각합니다. 도전하는 자세로, 새로운 것에 항상 궁금증을 가지는 과학자가 될 수 있도록 노력하겠습니다.

이 논문은 지금은 함께 할 수 없지만, 저를 세상에서 가장 자랑스럽게 생각해 주는 우리 엄마와 할머니께 바칩니다. 사랑합니다.

2016 년 6 월

이 종 주 배상

TABLE OF CONTENTS

LIST OF FIGURES

LIST OF TABLES

ABSTRACT

Epigenetic regulation of tumor progression and metastasis by chromatin remodeling factor SATB1

Jong-Joo Lee

Department of Medicine Science
The Graduate School, Yonsei University

(Directed by Professor Hyoung-Pyo Kim)

Special AT-rich sequence binding protein 1 (SATB1) is a nuclear protein that functions as a global chromatin organizer, regulating chromatin structure and gene expression. Recently, it has been reported that SATB1 is highly expressed in metastatic breast cancer cells and promotes growth and metastasis by reprogramming transcription profiles, suggesting SATB1 as a potential prognostic marker and therapeutic target for metastatic breast cancer. Although SATB1 is known to regulate hundreds of genes, it's binding to endogenous genes and regulation mechanism have rarely been demonstrated. In this study, we performed a systematic, genome-wide analysis of the functional significance of SATB1 in breast cancer cells. With the use of chromatin immunoprecipitation coupled with next-

generation sequencing (ChIP-seq), we identified around 20,000 SATB1-binding genomic regions. Also, we established epigenomic profiles for metastatic breast cancer cells using SATB1 loss-of-function system, and explored the role of SATB1 in the change of chromatin structure which is associated with gene expression. This comprehensive analysis of multiple epigenome data provides several novel SATB1-target genes which regulate growth and metastasis of breast cancer cells.

Key words: breast cancer, epigenetics, SATB1, chromatin immunoprecipitation, Histone modification, DNA methylation, genome-wide, biomarker

Epigenetic regulation of tumor progression and metastasis by chromatin remodeling factor SATB1

Jong-Joo Lee

Department of Medicine Science
The Graduate School, Yonsei University

(Directed by Professor Hyoung-Pyo Kim)

I. INTRODUCTION

Breast cancer is one of the most common malignant cancer and main cause of deaths from breast cancer is through metastases to distant organs.[1] Breast cancer also has heterogeneous feature, making it difficult not only to define its characters, but also to assess key factors for metastasis. Generally, breast cancer is classified by histological type, tumor grade, and lymph node status. Recent reports show that breast cancer could be grouped to at least four major molecular subtypes, which is luminal A, luminal B, HER2, and triple negative based on the presence or absence of predictive markers.[2,3]

Cancer development is a complicated mechanism involving reprogramming and progressive accumulation of abnormal multiple genes for its initiation, progression and metastasis.[4] During the development of cancer, epithelial cell characteristics of acquires

invasion, intravasation, evasion of immune system, extravasation and rapid proliferation through genetics and epigenetic events that represses tumor suppressor genes and promotes oncogenes induces to development cancer.[5] Metastasis is the last step of cancer development and its main characteristic is to move away from the primary tumor site which is the main cause of death in breast cancer patients.[6] The majority of metastasis studies were mainly focused on genetic mutation to form metastases, however with the increase in knowledge of epigenetics, epigenetic regulation such as chromosome structure, DNA methylation, histone modifications, and RNA mediated gene silencing have been identified as key factors to breast tumorigenesis.[7-10] Furthermore, the advent of gene expression profiling technology has brought new strategy understandings of breast cancer metastasis.[11]

Special AT-rich sequence-binding protein 1 (SATB1) is a chromatin remodeling protein expressed predominantly in thymus tissues.[12] SATB1 binds selectively to the nuclear matrix/scaffold-associating regions (MARs/SARs) which consists of ATC rich sequence.[12] The gene encoding SATB1 is located on chromosome 3p24.3 in the human genome and it consists of 763 amino acid (aa) or 85.9 kDa. SATB1 has three functional domains which consist of PDZ signaling domain in N-terminal, a two CUT domain (CD) in the center and homeodomain (HD) in the C-terminal region.[13,14] It was reported that the PDZ domain of SATB1 acts as dimerization or tetramerization and interacts with HDAC1,[15] β-catenin,[16] promyelocytic leukemia (PML),[17] PCAF/p300,[18] and CtBP.[19] CD and HD, also it is an essential element for specific DNA-binding acting as an anchor to accessible of transcription factors.[20]

After SATB1 was identified to be tissue specific, SATB1 was mainly investigated with T cell development and differentiation. During T cells have been determined its fate, SATB1 acts as dual role through distributes surrounding heterochromatin regions and tethers the specialized DNA sequences to recruits chromatin remodeling complex in thymus nuclei.[21-23] In development of T cell, SATB1 orchestrates higher order chromatin organization thereby modulating the expression of a vast number of genes and ultimately differentiates T helper 2 cells.[13,16,24,25] While SATB1 acts as a positive regulator in Th2 cells, maintaining Treg cell, SATB1 plays a critical role differentiating Treg that are essential for immune tolerance.[26,27] This process is accomplished by Foxp3, Foxp3, key master regulator of Treg, directly inhibiting SATB1 through binding at its promoter and indirectly inducing microRNAs which binds to the untranslated regions of SATB1.[26]

In 2008, SATB1, a high order chromatin organization and transcription regulator, was identified to promote tumor progression and metastasis in breast cancer.[28] The authors documented that SATB1 regulates global gene expression to bind at the target loci and recruit various coactivator and corepressor complex leading to the activation of oncogenes or inactivating tumor suppressor genes respectively.[28-30] This research suggests that SATB1 plays an important role as a master regulator to promote progression and metastasis in breast cancer and, therefore, can be considered a potential therapeutic target for metastatic breast cancer.

Since SATB1 has emerged as a critical factor in breast cancer, there has been an increase in reports on the relationship between SATB1 and the development of metastatic tumor in

various cancers such as bladder cancer,[31,32] colorectal cancer (CRC),[33-37] gastric cancer,[38,39] liver cancer,[40-42] ovarian cancer,[43-45] pancreatic cancer,[46,47] and prostate cancer.[48-50] However, SATB1 expression does not correlates with growth and development of tumor in small cell lung cancer (SCLC).[51-53] The role of SATB1 in tumorigenesis has subsequently been reported. Overexpression of SATB1 induced multidrug resistance and increased TNM stage.[54,55] Recently, the transcription factor FOXP3 known as a tumor suppressor in the breast and prostate epithelia, inhibited SATB1 expression via direct binding at SATB1 promoter and indirectly inducing miR-7 and miR-155 which binds to the 3'UTR of SATB1.[56] SATB1 was also identified as a mediator of Wnt signal which has an essential role in tumorigenesis.[34,37,57] Furthermore, SATB1 promotes cancer cell proliferation and invasion through the activation of MYC in pancreatic cancer.[58] Thus SATB1 has emerged as a master regulator in various biological processes including tumorigenesis.

Metastasis is the most common cause of death in cancer patients. However, the genetic and epigenetic mechanisms involved remains unclear. SATB1 is a unique chromatin organizer that modulates higher-order chromatin structure, leading to the regulation of various genes. However, the precise mechanism on how SATB1 changes chromatin and nuclear architecture, thereby regulating oncogenes and tumor suppressor genes is unclear. In this study we used knockdown system and integrated analysis of next generation sequencing system to demonstrate the role of SATB1 in breast cancer metastasis and its mechanism. Our results highlight an essential association between SATB1 and its target genes, as well as the mechanism of SATB1, which is a crucial metastasis regulator epigenetics.

II. MATERIALS AND METHODS

1. Cell culture

The breast cancer cell lines, MCF7, SKBR3, BT549 and MDA-MB-231 were maintained in Dulbecco's modified Eagle's (DMEM) (Welgene, Deagu, Korea) medium supplemented with 10% heat-inactivated fetal bovine serum (FBS) (Welgene), and 100 U/ml penicillin/streptomycin (Welgene).

2. Lentivirus shRNA vector construction and gene transduction

The shRNAs were designed, based on the SATB1 sequence (NM_002971): shRNA-SATB1 5'-GGATTTGGAAGAGAGTGTC-3' and the UCA1 sequence (NR_015379): shRNA-UCA1 5'-GAGAGCCGATCAGACAAACAA-3'. The oligoduplexes were cloned into pLKO.1-neo or pLKO.1-puro (Addgene, Cambridge, MA, USA), respectively, and transfected into 293FT cells using polyethylenimine (PEI) solution (Polysciences, Warrington, PA, USA). Virus-containing supernatants from the 293FT cells were collected after 48 - 72 hr incubation. Viral media was added to MDA-MB-231 cells with 8 ug/ml polybrene (Sigma-Aldrich, St Louis, MO, USA) and incubated overnight. 24 hr later, cells were sub-cultured with 1 mg/ml of G418 (Duchefa, Haarlem, The Nethelands).

3. Small interfering RNA transfection

24 hr prior to transfection, various number of cells were suspended in growth medium without antibiotics and seeded in a 6 well plate (SPL, Seoul, Korea). The cell density was 60-70% confluence at the time of transfection. Scrambled RNA (scRNA) and siRNA (Genolution, Seoul, Korea) were transfected with Lipofectamine RNAiMAX (Invitrogen, San Diego, CA, USA) according to the manufacturer's protocol. The sequences of siRNA is SATB1 5'- GAAGGAAACACAGACAUUA -3' and CAIX-1 5'- ACCUGAAGUUAAGCCUAAA -3' and CAIX-2 5'- GGCUGCUGGUGACAUCCUA -3'.

4. Quantitative real time polymerase chain reaction (real-time PCR)

Total RNA was isolated using Hybrid-R kit (GeneAll Biotechnology, Seoul, Korea), according to the manufacturer's protocol. Reverse transcription was performed with 1 μg of total RNA using the PrimeScript RT Kit (Takara, Shiga, Japan). Quantitative realtime-PCR was performed using the SYBR premix Ex Taq *II* (Takara) on the ABI StepOnePlus real-time PCR System (Applied Biosystems, Foster City, CA, USA) as follows: 95 ^{o}C (30 sec) for initial denaturation, 45 cycles at 95 ^{o}C (5 sec) and 60 ^{o}C (30 sec). Each sample was performed in duplicates reactions were analyzed for the expression of the gene of interest, and results were normalized to GAPDH mRNA. Primers sequences are listed in Table 1.

Table 1. Primer sequences used for real-time PCR

Gene	Forward (5' to 3')	Reverse (5' to 3')
GAPDH	GCACCGTCAAGGCTGAGAAC	ATGGTGGTGAAGACGCCAGT
SATB1	GTGGAAGCCTTGGGAATCC	CTGACAGCTCTTCTTCTAGTT
CLDN1	CCCCAGTGGAGGATTTACTCCTA	GCAATGTGCTGCTCAGATTCA
INHBA	GGAGGGCAGAAATGAATGAA	CCTTGGAAATCTCGAAGTGC
ADAMTS6	CCTGGGTTCAGCTTTTACCA	ATGACCTTTCGTCCCACAAG
CLSPN	GAGTCAGAAGCCAGGTGGAG	TGACTGTCCTCCCCAATTTC
S100A4	GATGAGCAACTTGGACAGCAA	CTGGGCTGCTTATCTGGGAAG
TGFB1	CAACAATTCCTGGCGATACCT	GCTAAGGCGAAAGCCCTCAAT
VEGFB	GAGATGTCCCTGGAAGAACACA	GAGTGGGATGGGTGATGTCAG
OASL	TTTCTGAGGCAGGAGCATTT	GCCCACCTTGACTACCTTCA
CAIX	CACTCCTGCCCTCTGACTTC	AGAGGGTGTGGAGCTGCTTA
UCA1	CGGGTAACTCTTACGGTGGA	TGGTCCATTGAGGCTGTAGA

5. Western blot analysis

Whole lysate was isolated using lysis buffer (50 mM Tris–HCl, pH 7.4, 1 mM EDTA, 0.1% SDS, 140 mM NaCl, 0.2% deoxycholic acid, and 2% triton X-100) with protease inhibitor cocktail (Sigma-Aldrich). Proteins were separated on sodium dodecyl sulfate (SDS)–polyacrylamide gels and transferred to polyvinylidene fluoride (PVDF) membranes (Invitrogen, San Diego, CA, USA). After blocking with skim milk, the membrane was incubated with the antibodies, followed by incubation with the horseradish peroxiadase-conjugated secondary antibody. Western blot analysis were performed using antibodies against SATB1 (BD Biosciences, San Jose, CA, USA), E-cadherin (BD Biosciences), N-cadherin (BD Biosciences), Slug (Cell Signaling), CAIX (Abcam, Cambridge, MA, USA) and β-actin (Sigma-Aldrich) as an internal control. The membranes were developed with SuperSignal West Femto Maximum Sensitivity substrate (Thermo Scientific, Rockford, IL, USA) and then analyzed using an LAS-4000 imaging system (GE Healthcare, Piscataway, NJ, USA).

6. Cell growth assay

In vitro proliferation was measured by seeding approximately 5 x 10^4 cells on 24-well plates (SPL). At specific time points, cells were isolated by incubation with 0.05% trypsin-EDTA (Invitrogen) for 5 min before counting. Trypan blue (Invitrogen) exclusion analysis indicated that 99–100% of the cells were viable.

7. Quantitation of apoptosis by Annexin V flow cytometry

Cells were washed twice with phosphate buffered saline (PBS) and resuspended in 1x binding buffer (10 mM HEPES, pH 7.4, 140 mM NaCl and 2.5 mM CaCl2). Afterwards, cells were incubated with 4 μl Annexin V-APC (e-Bioscience, San Diego, CA) and 4 μl of 100 μg/ml propidium iodide (Sigma-Aldrich) for 15 min at room temperature and then analyzed by flow cytometry using an FACSverse (BD Biosciences). Data analysis was performed using FlowJo software (Treestar, Ashland, OR, USA). Triplicate experiments were performed.

8. Transwell assay

Assessment of the metastatic potential of SATB1 in breast cancer cells *in vitro* was performed using Matrigel Invasion Chamber (BD Biosciences). Transwell was coated with matrigel or collagen. Cells then were seeded onto the upper chamber at a density of 5 x 10^4 cells per 100 μl per chamber and maintained in serum-free medium, and lower chambers were filled with 700 μl complete medium. Cells were incubated for 24 hr at 37 °C in a 5% CO2 incubator. Non-invaded cells retained on the upper surface were removed by scrubbing with a cotton swab. The invaded cells were fixed and stained with Hematoxylin and Eosin (H & E) staining. Four random fields were counted under a light microscope (Olympus, Tokyo, Japan). Digitized pictures were analyzed by Image J software (NIH, Bethesda, MD, USA). Experiments were performed in triplets.

9. Wound healing assay

Cells were plated in individual wells of six-well culture plates that form a monolayer on the dish surface. After 24 and 48 hr, a wound was generated in the monolayer of cells by completely scratching the cells in a line with a 200 μl pipette tip. Cells were washed with PBS and incubated in a fresh serum-free medium. The time of the scratching wound was designated as time 0. After 24 and 48 hr, migration of cells into the wound was recorded under a light microscope (Olympus). Digitized pictures were analyzed by Image J software (NIH). Experiments were performed in triplets.

10. Plasmid constructs

To generate the luciferase reporter constructs, CAIX and UCA1 promoter regions subcloned into pGL3-Basic luciferase reporter vector (Promega, Madison, WI, USA). Primers sequences are listed in Table 2.

11. Transient transfections and luciferase assays

The transient transfections of MDA-MB-231 cells were performed using PEI solution. After 24 hr, luciferase activities were analyzed using a luminometer (TD-20/20 luminometer, Turner Designs, Sunnyvale, CA, USA) and a dual luciferase assay system kit (Promega).

Table 2. Primer sequences used for plasmid construction

Location	Direction	Sequence (5' to 3')
CAIX promoter	Forward	AGGGTACCCTTGGGTTCCAAGCTGAGTC
	Reverse	TCGAGCTCAACTTCAGGGAGCCCTCTTC
UCA1 promoter	Forward	CAGCTAGCTCTCAGGCTGT
	Reverse	GACTCGAGCAGGGTCGATTG
UCA1 -3.0 kb	Forward	TCGGTACCGAAAGTGTTAAACAAAACTT
	Reverse	CTACGCGTTAAGAACTCCTGCTTT

12. Measurement of extracellular pH

Cells were plated in 60 mm dish and allowed to recover overnight. When cells form a monolayer on the dish surface, it changes by fresh DMEM media. Then, cells were incubated under normoxia or hypoxia for 24 hr. After 24 hr, media was collected and pH was measured immediately by a pH meter (Eutech Instruments, Singapore)

13. RNA-sequencing followed by Next-generation sequencing (NGS)

To analyze Illumina Hiseq-2000, the sequencing library was performed using Illumina ® TruSeq™ RNA Sample Preparation Kit (Illumina, San Diego, CA, USA), according to the manufacturer's protocol. The amplificated RNA assessed and quantified using Bioanalyzer (Agilent Technologies, Santa Clara, CA, USA). The resulting libraries were sequenced on an Illumina Hiseq-2000 (Illumina), according to the manufacturer's instructions. The raw data were checked quality using NGSQCToolkit v2.3 (quality score > 20).[59]

14. Chromatin Immunoprecipitation (ChIP) followed by Next-generation sequencing (NGS)

Cells were incubated for 10 min at room temperature in tissue culture medium containing 1% formaldehyde (Sigma-Aldrich). The reaction was quenched by addition of glycine to 125 mM and incubated for 5 min at room temperature. Cells washed in PBS, then pelleted, and lysed in buffer A (5 mM PIPES, pH 8.0, 85 mM KCl, and 0.5% NP40) for 10 min on ice.

Nuclei were pelleted and washed in buffer A without NP40, then lysed in nuclei lysis buffer (10 mM Tris-HCl, pH 8.0, 2 mM EDTA, 1 mM PMSF and 0.2% SDS). Lysed nuclei were sonicated using a bioruptor sonicator (Diagenode, Seraing, Belgium) until the average DNA fragment was ~500 bp. Chromatin samples were diluted in 2× RIPA-B buffer (10 mM Tris-HCl, pH 8.0, 2% Triton X-100, 0.2% deoxycholic acid, and 280 mM NaCl) followed by immunoclearing with 50 μg BSA, and secondary antibodies linked to magnetic beads (Dynal, Lake Success, NY, USA). Immunoprecipitations were performed with 5 μg primary antibody to SATB1 (BD Biosciences), anti-H3K4me1 (Abcam), anti-H3K4me3 (Abcam), anti-H3K27me3 (Abcam) and anti-H3K27Ac (Abcam) overnight at 4°C. Immune complexes were harvested with secondary antibodies linked to magnetic beads, and washed twice for 5 min in each of the following buffers: RIPA-140 buffer (10 mM Tris-HCl, pH 8.0, 0.1% SDS, 1% Triton X-100, 1 mM EDTA, 0.1% deoxycholic acid, and 140 mM NaCl), RIPA-300 buffer(10 mM Tris-HCl, pH 8.0, 0.1% SDS, 1% Triton X-100, 1 mM EDTA, 0.1% deoxycholic acid, and 300 mM NaCl), and LiCl buffer(10 mM T Tris-HCl, pH 8.0, 250 mM LiCl, 0.5% NP40, 1 mM EDTA, and 0.5% deoxycholic acid), followed by a final wash with TE (10 mM Tris-HCl, pH 8.0 and 1 mM EDTA). Immune complexes were disrupted with elution buffer (100 mM NaHCO3 and 1% SDS), and cross-links were reversed by adding NaCl to a final concentration of 200 mM and RNase A incubated at 37°C and by adding proteinase K overnight at 65°C. DNA was purified by phenol/chloroform (Sigma-Aldrich extraction, and ethanol precipitated. DNA pellets were dissolved in 50 μl water, and 2 μl were used as template for PCR reactions using StepOneplus real-time PCR System (Applied

Biosystems). Primers sequences are listed in Table 3. To prepared libraries, samples were amlified using paired-end Illumina primers, then amplificated DNA assessed and quantified using Bioanalyzer(Agilent Technologies). The resulting libraries were sequenced on an Illumina Hiseq-2000(Illumina), according to the manufacturer's instructions. The raw data were checked quality using NGSQCToolkit v2.3 (quality score > 20).[59]

Table 3. Primer sequences used for ChIP assay

Location	Direction	Sequence (5' to 3')
INHBA	Forward	AGGATCCGAGGGGCACAG
	Reverse	GCTGAGAGTTGGGTACATCC
GAPDH	Forward	CGGCTACTAGCGGTTTTACG
	Reverse	GCTGCGGGCTCAATTTATAG
CAIX -4.0 kb	Forward	CAGAGTGTACCCTGGACCAC
	Reverse	ACCTCAGATGTAGTCAGCCT
CAIX -0.3 kb	Forward	GGCCAGGGTTAGCTGAGG
	Reverse	CCATGGACTCAGCTTGGAAC
CAIX TSS	Forward	TTTCCAATGCACGTACAGCC
	Reverse	CCGGGATCAACAGAGGGAG
CAIX +0.1 kb	Forward	CTCACTGTGCAACTGCTGCT
	Reverse	GTCATCTTCCCCAGAAGAGC
UCA1 -3.0 kb	Forward	ATGAGAGGCCACTGTTTTGG
	Reverse	GAGGATTTGCCTCCTTCCTT
UCA1 +0.8 kb	Forward	TTCACTTTGGGCAATCTTCC
	Reverse	TTATATTGCGGCCAAGCAGT
UCA1 +7.7 kb	Forward	CACACTCAGCATTTCCGGC
	Reverse	TTTGGGGTTTGGGGTCTTTG

15. MBD assay followed by Next-generation sequencing (NGS)

Cells isolated using DNeasy Blood and Tissue kit (Qiagen, Valencia, CA, USA). 5 μg DNA isolated was sonicated to ~100-500 bp with Covaris (Covaris, Woburn, MA,USA). Fragmented DNA were performed using MethylMiner Methylated DNA Enrichment Kit, (Invitrogen), according to the manufacturer's protocol. To prepared libraries, samples were amlified using paired-end Illumina primers, then amplificated DNA assessed and quantified using Bioanalyzer. The resulting libraries were sequenced on an Illumina Hiseq-2000 (Illumina), according to the manufacturer's instructions. The raw data were checked quality using NGSQCToolkit v2.3 (quality score > 20).[59]

16. Bioinformatic data analysis

In RNA-seq, we used RSEM[60] and EBSeq[61] to identify DEGs (differentially expressed genes). High-quality reads were mapped to Human reference (build hg19) genome using RSEM's *rsem-calculate-expression* function with bowtie2 v2.0.0-beta7[62] and the expression levels of each transcript were quantified as FPKM (fragments per kilobase of exon per million fragments mapped). FPKM values were passed to EBSeq using RSEM's *rsem-run-ebseq* function. DEGs were defined as $|\log_{10} FC| \geq 1$ and $p < 0.05$. The RNA-seq data were visualized using University of California, Santa Cruz (UCSC) Genome browser.[63] In ChIP-seq, High-quality reads were mapped to Human reference (build hg19) genome using Bowtie2 v2.0.0-beta7[62] with the option: bowtie2 --mp 1,1 --np 1 --score-min L,0,-0.1.

Differential binding sites were identified by counting the number of mapping reads. Read counts were calculated for each gene in the 3kb region surrounding the TSS using HTSeq v0.6.1[64] and were converted log2 CPM (count per million) values using Bioconductor package edgeR v3.6.8.[65] To eliminate biases between libraries, normalization was performed using the TMM (trimmed mean of M-values).[66] The ChIP-seq data were visualized using UCSC Genome browser.[63] To calculate ChIP signal in surrounding promoter region, mapped reads were converted into Tag directories using HOMER and promoter regions are split into 50 equally sized bins. Tag enrichment profiles were generated using HOMER and normalized to 10million tags. MACS v1.4.2 was used to call significant SATB1 binding peaks, with default parameters. To discovery de novo motif enriched around the peaks was carried out using MEME. Peaks separated with PeakSplitter were used.

17. Gene Ontology

GO enrichments analysis was done using the online functional annotation tools gene set enrichment analysis (GESA).[67]

18. Statistical analysis

Results are expressed mean ±S.D. Statistical analysis is as performed by student's t-test. Relationships were considered statistically significant when *p-value* was less than 0.05.

III. RESULTS

1. Expression of SATB1 in breast cancer cell

To examine the role of SATB1 in breast cancer cell lines, we observed SATB1 expression in various breast cancer cell lines. As previous study reported, SATB1 mRNA and protein were higher in triple negative (TN) breast cancer cells than in other breast cancer cells.[28] We also observed that SATB1 mRNA and protein levels were significantly higher in BT549 and MDA-MB-231 cells than in MCF7 and SKBR3 cells, as previously described (Figure 1A-B). When cells acquire malignant properties, epithelial cells transforms to a mesenchymal phenotype, process referred to as epithelial to mesenchymal transition (EMT).[68] To identify the correlation between cancer type and metastasis phenotype, we analyzed expression of E-cadherin and N-cadherin, known to mediate cell-to-cell adhesion as well as Slug, known to promote EMT in breast cancer. Whereas E-cadherin protein level observed in non-aggressive cancer cell, expression of N-cadherin and Slug, which are EMT markers, were detected in aggressive cancer cells (Figure 1B). Together, these observations indicate that SATB1 expression correlates with poor prognosis in breast cancer. Therefore, we selected MDA-MB-231 as the model cell line for this experiment.

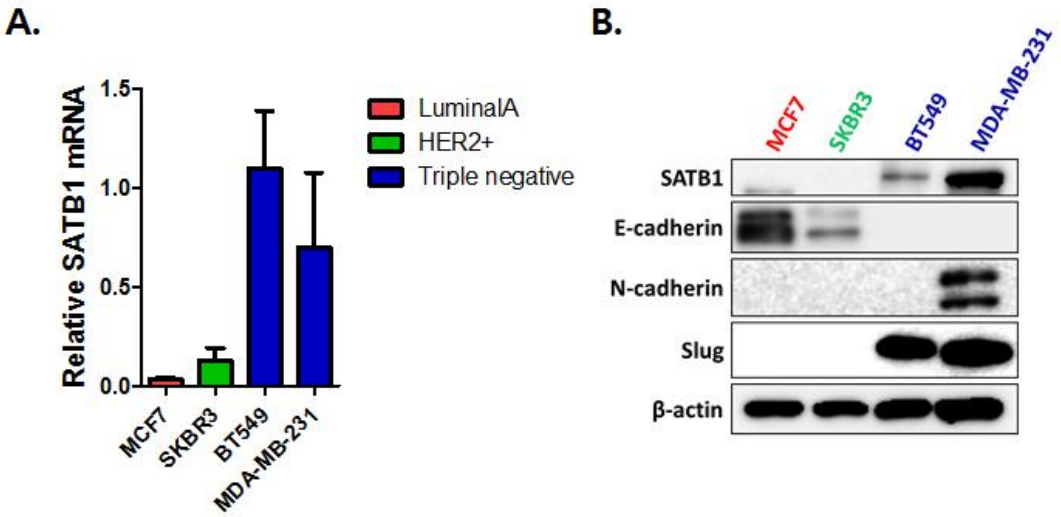

Figure 1. SATB1 mRNA and protein expression in breast cancer cells. A. mRNA of SATB1, relative to GAPDH, was quantitated by real-time PCR. For each sample, the bar indicates S.D from three experiments. B. Whole cell lysates were separated with SDS/PAGE and subjected to Western blot analysis using antibodies to SATB1, E-cadherin, N-cadherin, Slug and β-actin as an internal control.

2. SATB1-diminished in MDA-MB-231 cells exhibits reduced tumorigenic phenotype

Previous study reported that knockdown of SATB1 in aggressive breast cancer cell reverse metastatic phenotype.[28] To confirm this study, we generated a MDA-MB-231 cells with diminished SATB1 using shRNA construct. Depletion of endogenous SATB1 in MDA-MB-231 cells was confirmed by real-time PCR and western blot. These results showed decreased SATB1 mRNA and protein level (Figure 2A-B). Furthermore, siRNA mediated knockdown of SATB1 also affected mRNA and protein level (Figure 2C-D).

Next, we investigated the potential role of SATB1 in breast tumorigenesis *in vitro*. To determine whether SATB1 expression affects cell proliferation, we measured cell growth every two days. SATB1 inhibited cell growth and proliferation (Figure 3A). In addition, SATB1 Knockdown by shRNA in MDA-MB-231 cells affected apoptosis (Figure 3B). We then examined whether SATB1 expression associated with cell invasion and migration. Using transwell assay and scratch wound healing assay, we found that SATB1 inhibited breast cancer cell invasion and migration (Figure 3C-E). Collectively, these data indicate that shRNA-mediated SATB1 Knockdown reduced the potential tumorigenicity of aggressive breast cancer cells.

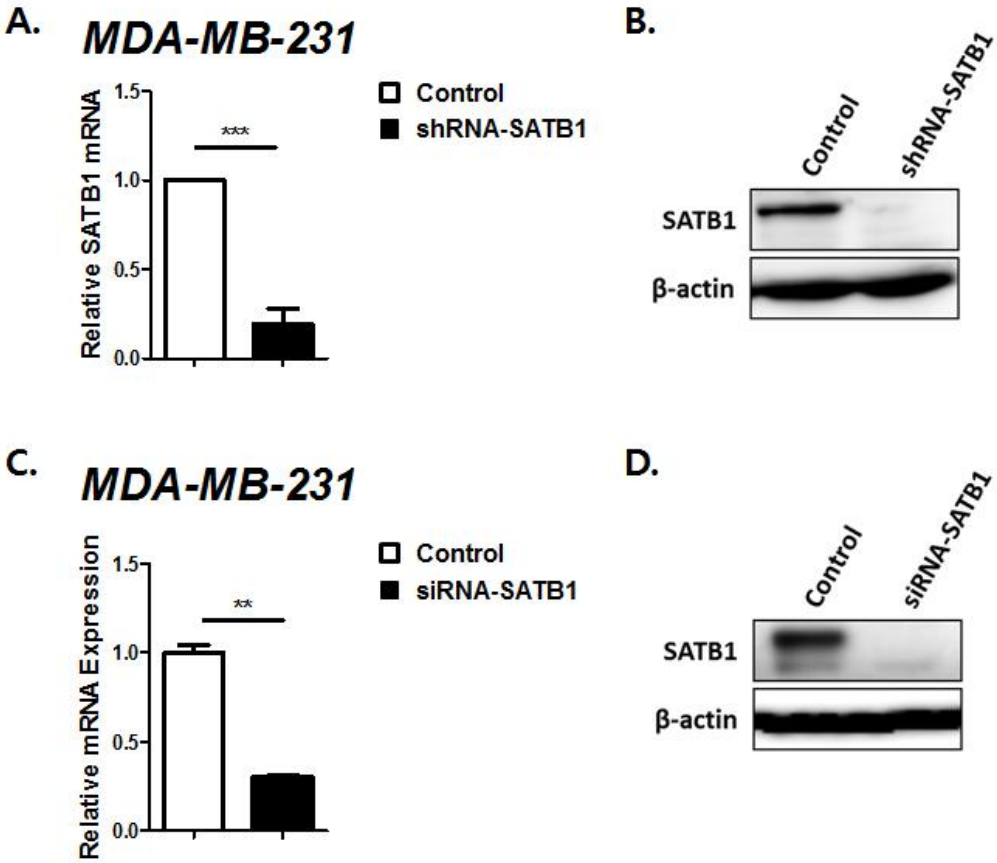

Figure 2. Generation of loss-of function SATB1 in MDA-MB-231 cells using shRNA and siRNA system. A. MDA-MB-231 cells transduced with lentiviruses expressing SATB1 shRNA or containing empty LKO vector. Positive cells were selected with G-418. mRNA of SATB1, relative to GAPDH, were quantitated by real-time PCR. For each sample, the bar indicates S.D from three experiments. B. SATB1 protein levels were determined by western blot. C. Quantitative real-time PCR was used to measure the relative mRNA levels of SATB1 in SATB1 siRNA-transfected MDA-MB-231 cells. For each sample, the bar indicates S.D from three experiments. D. Western blot was used to measure the protein level of SATB1.

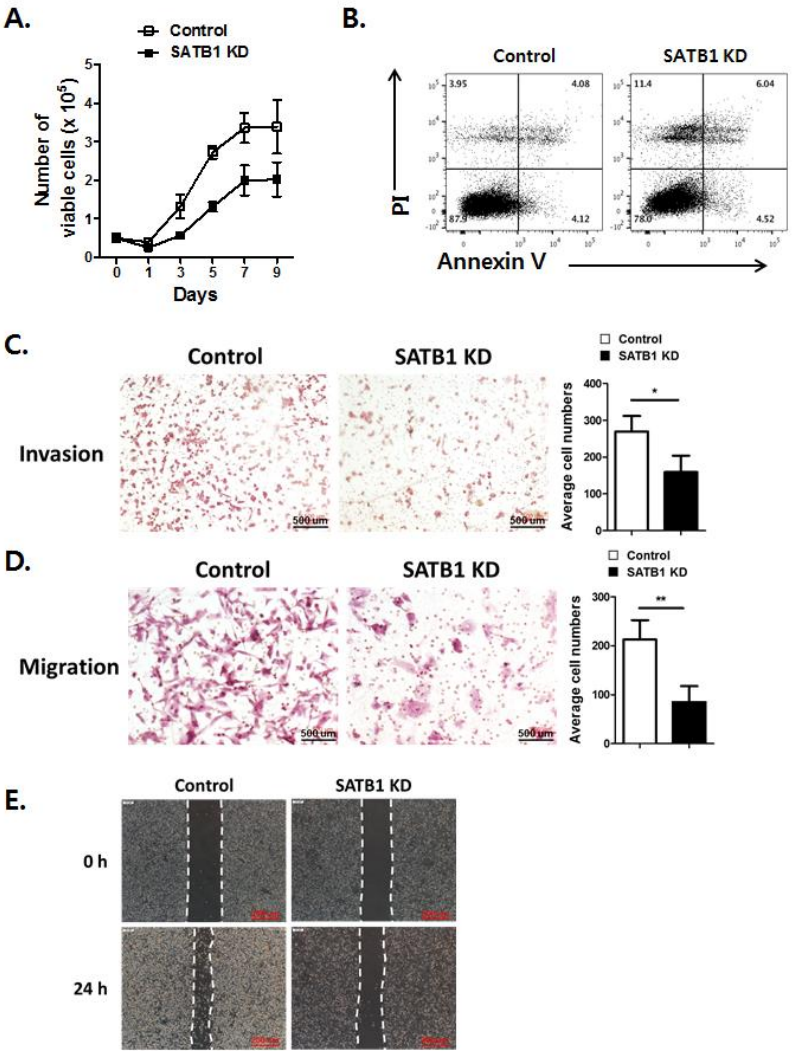

Figure 3. Effect of SATB1 tumor growth and aggressiveness in breast cancer. A. Viability of cells were counted after trypan blue staining. B. Flow cytometric analysis of apoptotic cells after infection of shRNA or control. C and D. Transwell invasion and migration assay of MDA-MB-231 cells infected with shRNA-SATB1. E. Scratch wound healing assay of SATB1 knockdown cells. For each sample, the bar indicates S.D from three experiments.

3. Effect of SATB1 on global gene expression profile in MDA-MB-231

To identify SATB1 regulated genes in metastatic breast cancer cells, we performed genome-wide mapping for transcriptome. To analyze RNA profiling by SATB1, we used RSEM and EBSeq web-based analysis program (Figure 4A, Table 4). Differentially expressed genes (DEG) were called with EBSeq, using 2 fold change and a *p-value* cutoff < 0.05 (Figure 3C). Among the DEG, 222 genes including CLDN1, INHBA, ADAMTS6 and CLSPN were downregulated by SATB1, and 470 genes including S100A4, TGFB1, VEGFB and OASL were upregulated by SATB1. We validated these genes by real-time PCR (Figure 3D). The result of RT-PCR confirmed the expression patterns which correlated with RNA-seq analyzed data. To globally assess the changes in SATB1 mediated transcriptome, we analyzed the differentially expressed genes with gene set enrichment analysis (GESA).[67] The GESA data revealed that the gene sets involved in E2F targets, G2M checkpoint, small cell lung cancer and cell cycle were downregulated by SATB1 genes, whereas the gene sets involved in p53 pathway, Interferon gamma response, hypoxia, antigen processing and presentation, asthma and MAPK signaling pathway were upregulated by SATB1 genes (Table 5).

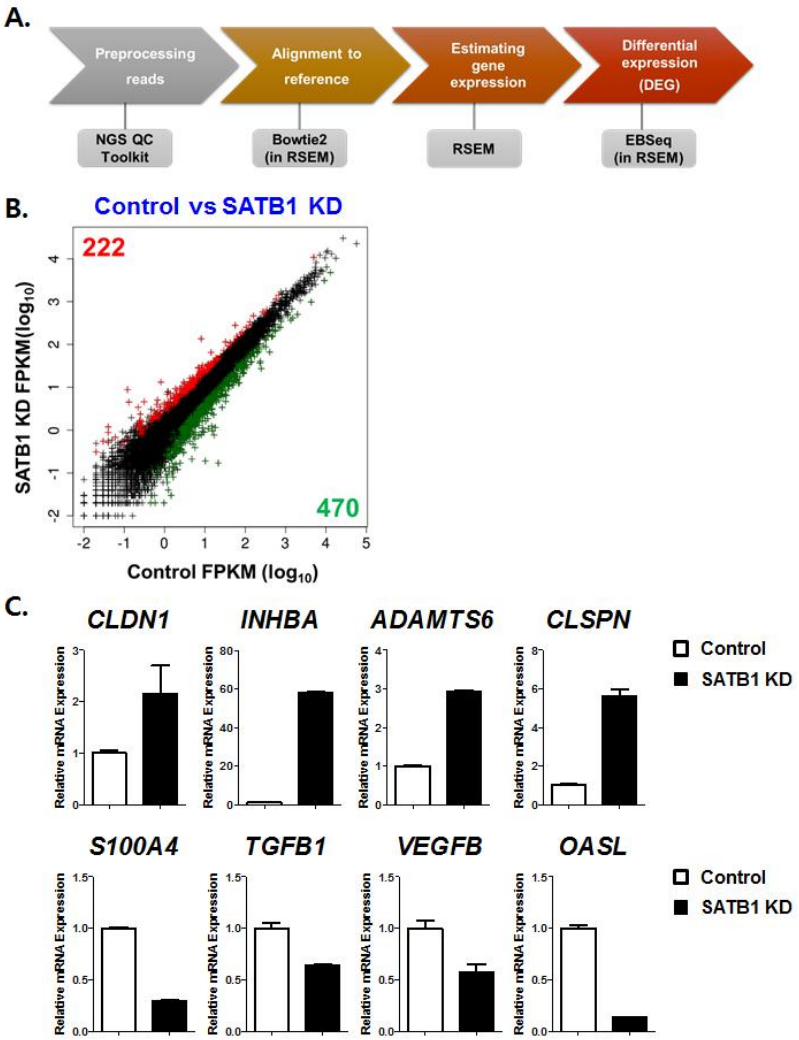

Figure 4. Genome-wide analysis of gene expression by RNA-seq. A. Schematic representation of RNA-sequencing analysis workflow. B. Scatter plots of DEG pattern. Significant gene (Fold change > 2, *p-value* < 0.05) downregulated by SATB1 are shown in red, and upregulated by SATB1 are shown in green. C. Validation of RNA-seq data by real-time PCR analysis. Each mRNA, relative to GAPDH, was quantitated by real-time PCR. For each sample, the bar indicates S.D from three experiments.

Table 4. Summary of RNA-seq mapping statistics

	Control	SATB1 KD
Total number of reads	28,119,776	30,992,656
Total number of HQ reads	24,957,250	28,002,762
Unique mapped read number	5,261,888	5,768,782
Overall alignment rate	74.37%	73.51%
Average read length (base)	101	101

Table 5. Gene ontology analysis of SATB1 target genes

Downregulation by SATB1

Gene set	Number of genes	Normalized enrichment score (NES)	*p-value*[1]
E2F TARGETS	15	3.27	0.00
G2M CHECKPOINT	12	2.50	0.00
SMALL CELL LUNG CANCER	11	2.10	0.01
CELL CYCLE	9	2.07	0.01

[1] *p-value* < 0.05

Upregulation by SATB1

Gene set	Number of genes	Normalized enrichment score (NES)	*p-value*[1]
P53 PATHWAY	27	-2.17	0.00
INTERFERON GAMMA RESPONSE	22	-1.89	0.00
HYPOXIA	39	-1.87	0.01
ANTIGEN PROCESSING AND PRESENTATION	17	-2.23	0.00
ASTHMA	7	-2.06	0.00
MAPK SIGNALING PATHWAY	12	-2.05	0.00

[1] *p-value* < 0.05

4. Effect of SATB1 on genome-wide histone modifications in MDA-MB-231

To identify whether SATB1 affected histone modification, we performed chromatin immunoprecipitation (ChIP) coupled with high-throughput sequencing (ChIP-seq) using antibody that recognized H3K4me3 which is an active marker, and H3K27me3 which is a repressor marker. To analyze ChIP-seq, we used HTseq for counting mapped reads and edgeR for searching differential ChIP signals (Figure 4A). The reads mapped to an overall alignment rate of 98.76% and 98.48% enrichment of H3K4me3 in the control and SATB1 knockdown, respectively (Table 6). Next we explained the distribution profiles of H3K4me3. We found that H3K4me3 peaks were usually distributed in the promoter regions (Figure 4B). To understand the correlation between H3K4me3 and expression, we systematically calculated the enrichment of H3K4me3 3 kilobase (kb) upstream and downstream from transcription start sites (TSS) in all the genes, and compared them with relative gene expression categorized based on RNA-seq. As expected, increased enrichment of H3K4me3 correlated with genes expression (Figure 4C-D).

To define SATB1 regulation of enriching of H3K4me3, we compared differential H3K4me3 signals between control and SATB1 knockdown. We found that 2975 genes were decreased by SATB1, however 1,408 genes were increased by SATB1 (Figure 6A).

Furthermore, we analyzed ChIP-seq for H3K27me3, referred to a global repression mark. The overall alignment rate of control and SATB1 knockdown revealed 98.30% and 97.83% respectively (Table 7). According to the analysis, the major H3K27me3 peaks were in the intron and intergenic regions (Figure 7A). In addition, we examined the correlation between

gene expression and enrichment of H3K27me. As a result, occupancy of H3K27me3 was slightly decreased according to active gene expression (Figure 7B). This was confirmed though the genome browser (Figure 7C). In conclusion, the presence of H3K27me3 commonly revealed in the intron and intergenic regions were absenct of RNA-seq reads. We identified that SATB1 changes a large number of histone modification (Figure 8A).

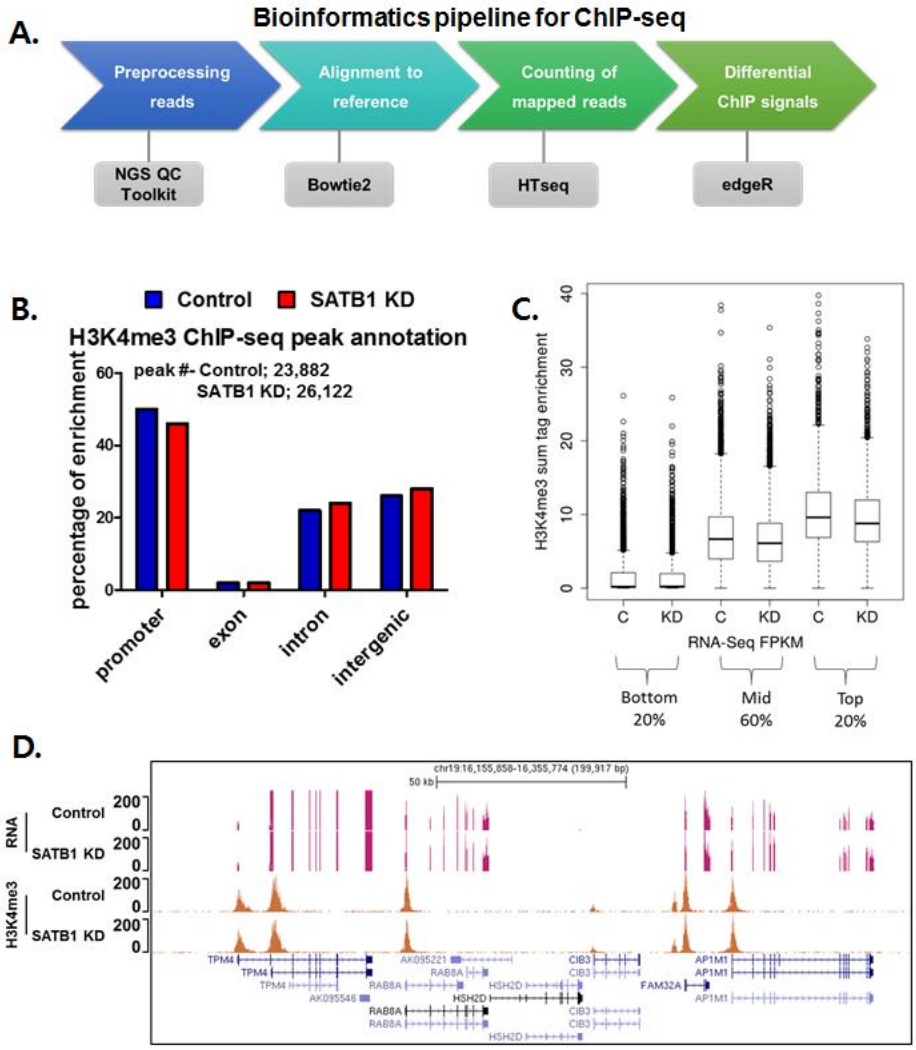

Figure 5. Distribution of H3K4me3. A. Schematic representation of ChIP-sequencing analysis workflow. B. The distribution of H3K4me3 was analyzed by location including promoter, exon, intron and intergenic regions. C. Genes were categorized based on increased expression levels. Enrichments of H3K4me3 were collected at corresponding genes. D. A snapshot of the representative genome browser shows the H3K4me3 ChIP-seq and RNA-seq reads.

Table 6. Summary of ChIP-seq for H3K4me3 mapping statistics

	Control	SATB1 KD
Total number of reads	25,980,124	28,018,440
Total number of HQ reads	21,115,610	23,060,782
Unique mapped read number	9,515,856 (90.13%)	10,380,197 (90.03%)
Overall alignment rate	98.76%	98.48%
Average read length (base)	101	101

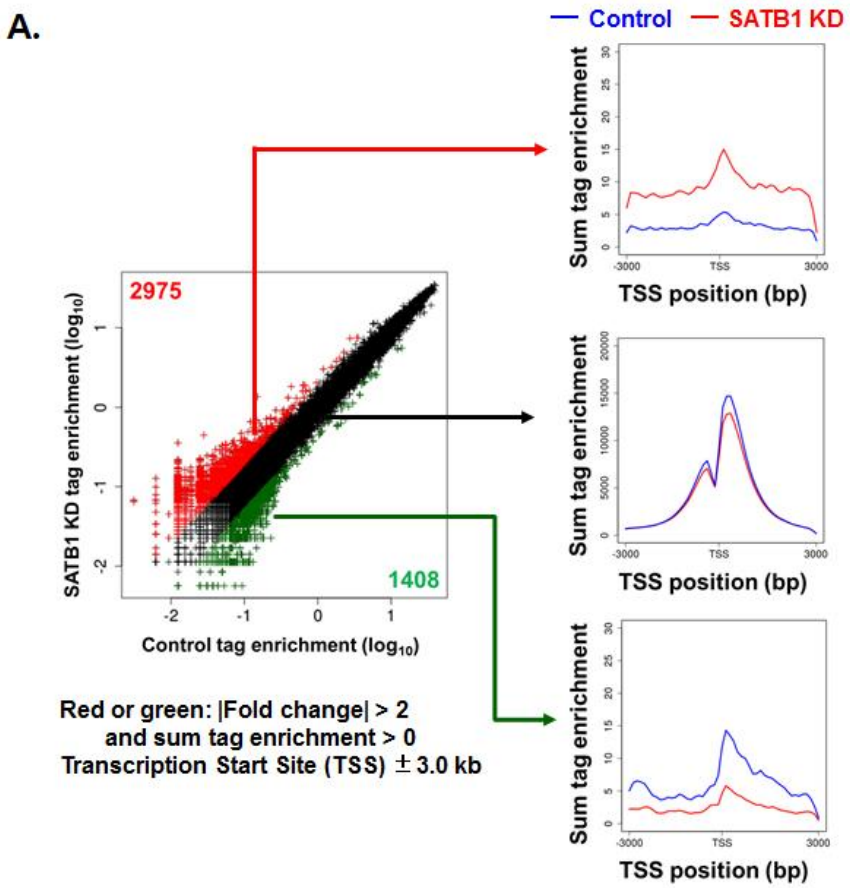

Figure 6. Regulation of H3K4me3 status by SATB1. A. The sum tag enrichment profiles for H3K4me3 across 3 kb upstream and downstream from the transcription start sites (TSS). Significant genes (Fold change > 2) downregulated by SATB1 shown in red, and upregulated genes by SATB1 shown in green.

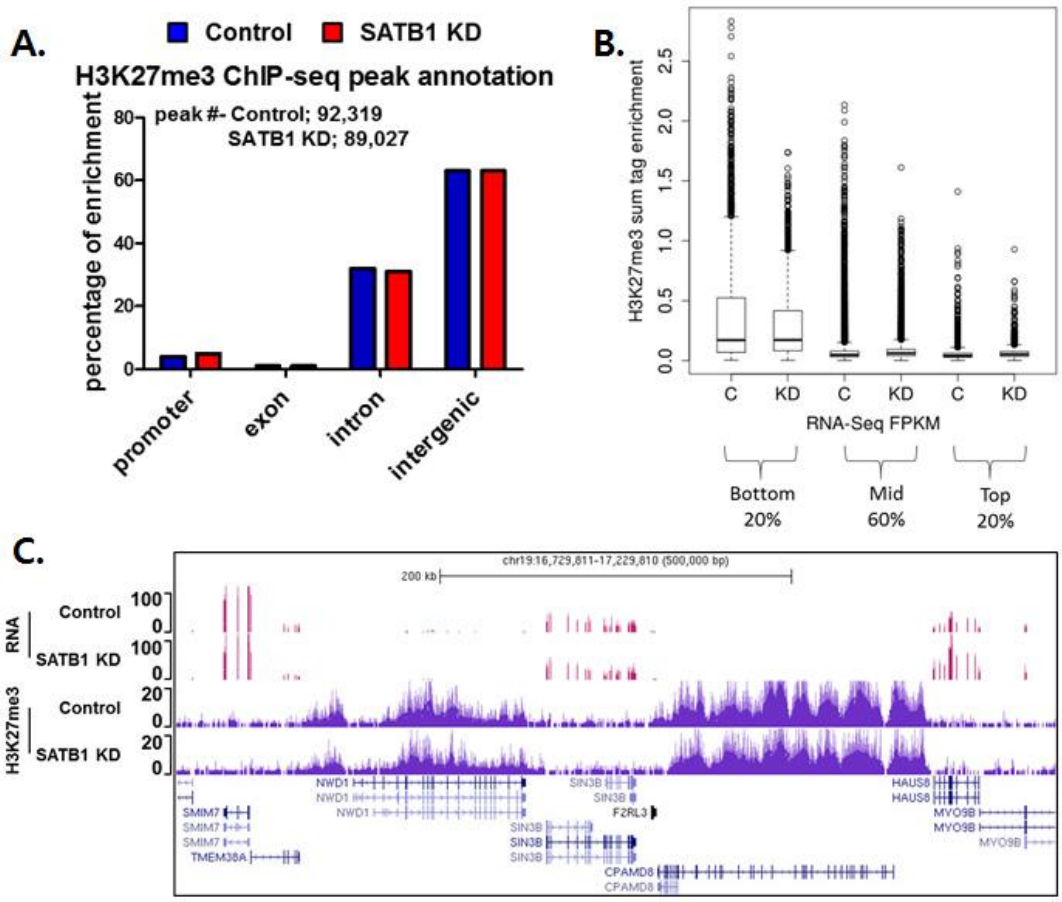

Figure 7. Distribution of H3K27me3. A. The distribution of H3K27me3 was analyzed based on the location including promoter, exon, intron and intergenic regions. B. Genes were categorized based on increased expression levels. Enrichments of H3K27me3 were collected at corresponding genes. C. A snapshot of the representative genome browser shows the H3K27me3 ChIP-seq and RNA-seq reads.

Table 7. Summary of ChIP-seq for H3K27me3 mapping statistics

	Control	SATB1 KD
Total number of reads	75,984,118	78,656,968
Total number of HQ reads	70,219,038	73,289,540
Unique mapped read number	30,853,631 (87.88%)	31,511,241 (85.99%)
Overall alignment rate	98.30%	97.83%
Average read length (base)	101	101

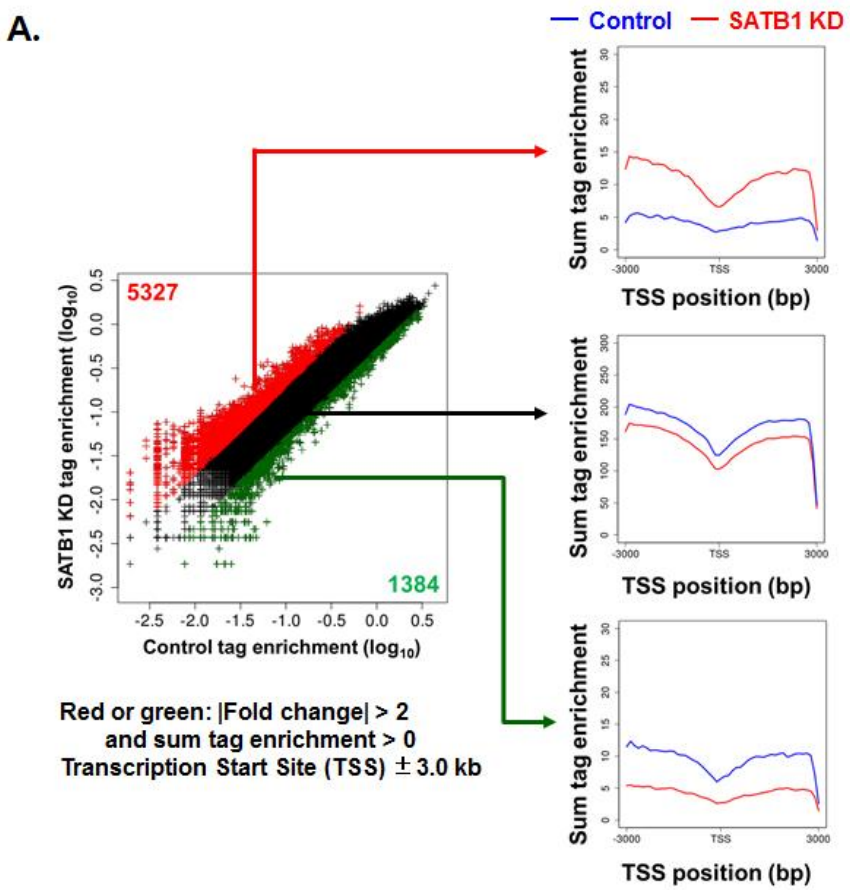

Figure 8. Regulation of H3K27me3 status by SATB1. A. The sum tag enrichment profiles for H3K27me3 across 3 kb upstream and downstream from the transcription start site (TSS). Significant genes (Fold change > 2) downregulated by SATB1 shown in red, and upregulated genes by SATB1 shown in green.

5. Effect of SATB1 on genome-wide DNA methylation in MDA-MB-231

Next, we investigated the effects of SATB1 based on DNA methylation status. We performed genome-wide mapping for DNA methylome in the control and SATB1 knockdown genome DNA. It was analyzed MBD-seq in the same pipeline that was used when analyzing the ChIP-seq (Figure 9A). We could read 27,028,576 of control methylated genomic DNA and 28,219,714 of SATB1-depleted methylated genomic DNA. Each read was performed quality testing using NGS QC toolkit, then we mapped 94.98% overall alignment rate of control and 94.88% for the overall alignment rate of SATB1-depleted sample (Table 8). To analyze differential methylation enrichment genes between control and SATB1 knockdown sample, we calculated the count per million (CPM) of genes through edgeR package. DNA methylation pattern was compared to the result of H3K27me3 ChIP-seq (Figure 9B). However, enrichment of DNA methylation did not relate to the gene expression (Figure 9C-D).

To define regulation of DNA methylation status by SATB1, we evaluated differential signals between control and SATB1 knockdown. Approximately 5,000 genes were changed, being either upregulated or downregulated by SATB1 (Figure 10A).

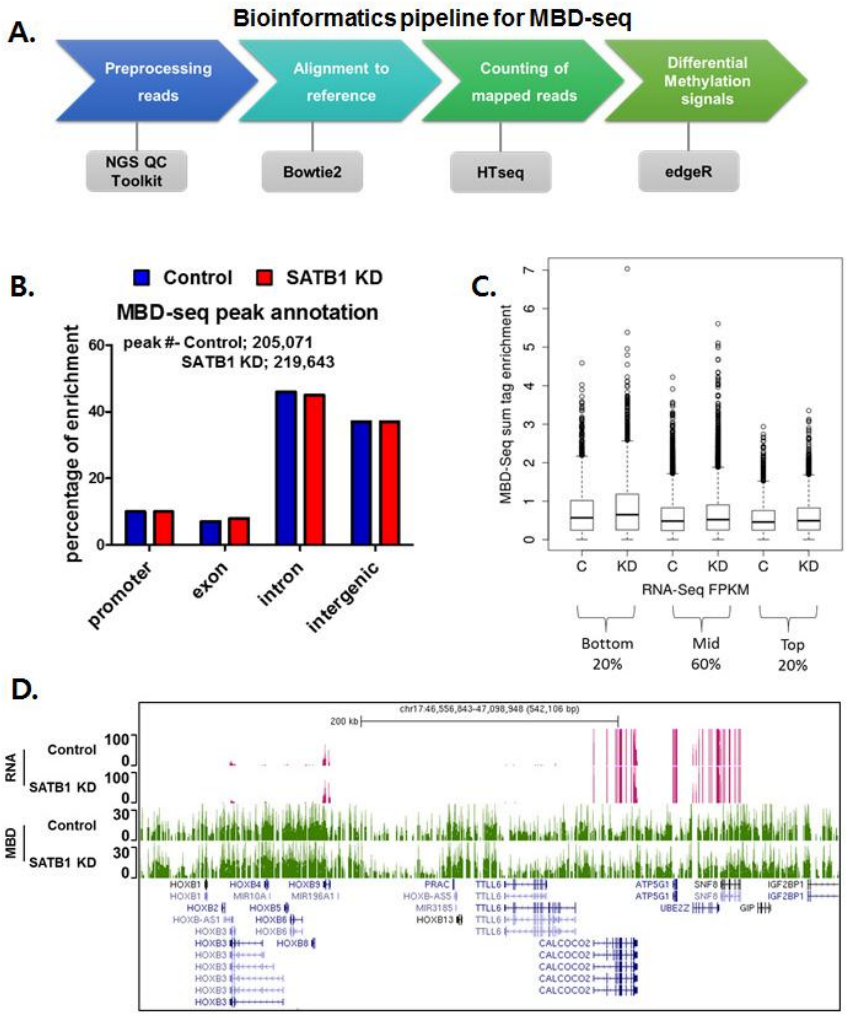

Figure 9. Distribution of DNA methylation. A. Schematic representation of MBD-sequencing analysis workflow. B. The distribution of DNA methylation was analyzed based on location including promoter, exon, intron and intergenic regions. C. Genes were categorized based on increasing expression levels. Enrichments of DNA methylation were collected within the corresponding genes. D. A snapshot of the representative genome browser shows the MBD-seq and RNA-seq reads.

Table 8. Summary of MBD-seq mapping statistics

	Control	SATB1 KD
Total number of reads	27,028,576	28,219,714
Total number of HQ reads	23,870,842	24,586,146
Unique mapped read number	8629590 (72.30%)	8268871 (67.27%)
Overall alignment rate	94.98%	94.88%
Average read length (base)	101	101

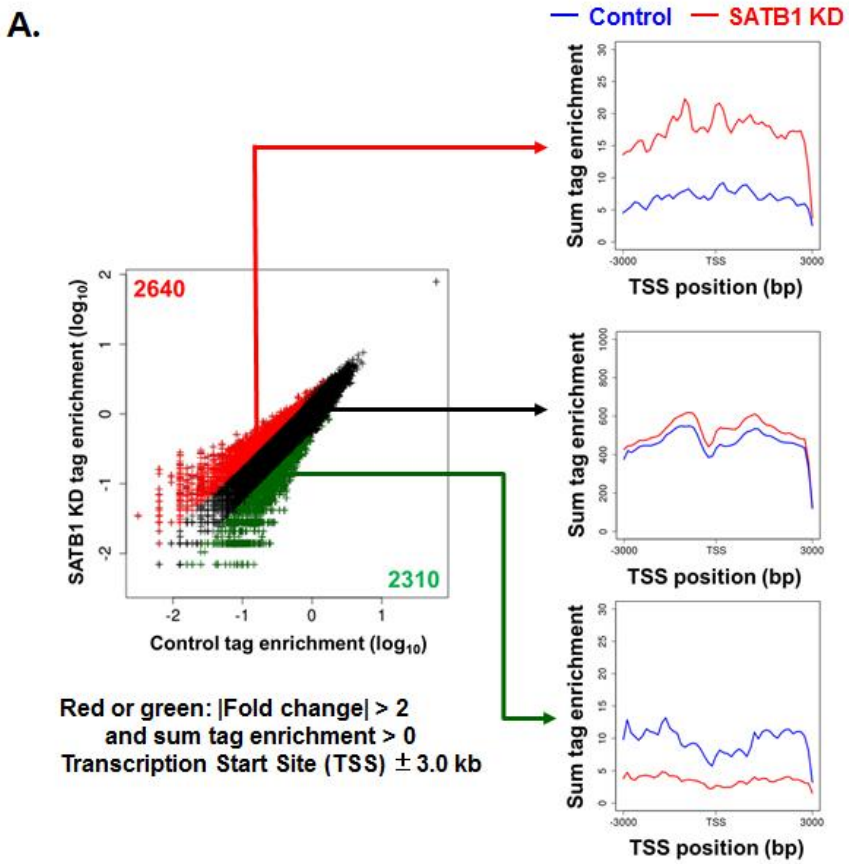

Figure 10. Regulation of DNA methylation by SATB1. A. The sum tag enrichment profiles for DNA methylation across 3 kb upstream and downstream from transcription starts (TSS) regions. Significant genes (Fold change > 2) downregulated by SATB1 shown in red, and upregulated genes by SATB1 shown in green.

6. Characterization of genome-wide SATB1 binding pattern in MDA-MB-231

Although previous studies demonstrated that SATB1 directly binds to its target genes, SATB1 binding site is not completely understood at a genome-wide level. To determine where SATB1 binds in the genomic DNA, we performed ChIP-seq against SATB1 protein in MDA-MB-231 cells It also was analyzed SATB1 ChIP-seq in the same pipeline that was used when analyzing the Chip-seq. (Figure 11A). We read 37,735,874 genomic DNA through high-throughput sequencing and aligned 96.07% overall alignment rate for SATB1 ChIP (Table 9). We counted 36,336 SATB1 peaks in MDA-MB-231 cells. As a result of genomic distribution of SATB1 binding peaks, we found that peaks were distributed at the intron and intergenic regions (Figure 11B-D). Analysis of best-scored ChIP peaks by MEME predicted a major consensus sequence (Figure 11C). These data correlated with previous study which reported that SATB1 binds to the matrix attachment region which consists of mixed A's, T's and C's excluding G's.[12] Validating the quality of our result of SATB1 ChIP-seq, the result was confirmed by SATB1 ChIP and real-time PCR. As a result, our analysis and experiment data showed correlation (Figure 11E).

To gain insights into the comprehensive epigenomic profiling, we have RNA-seq data, ChIP-seq data for histone modification and SATB1, and MBD-seq data (Figure 12A). Through these datas, we discovered that H3K4me3 peaks were detected in actively expressed genes, however H3K27me3 peaks were detected in repressed genes and DNA methylation peaks were mostly detected in the gene body of active genes. Furthermore we identified genome-wide SATB1 binding sites.

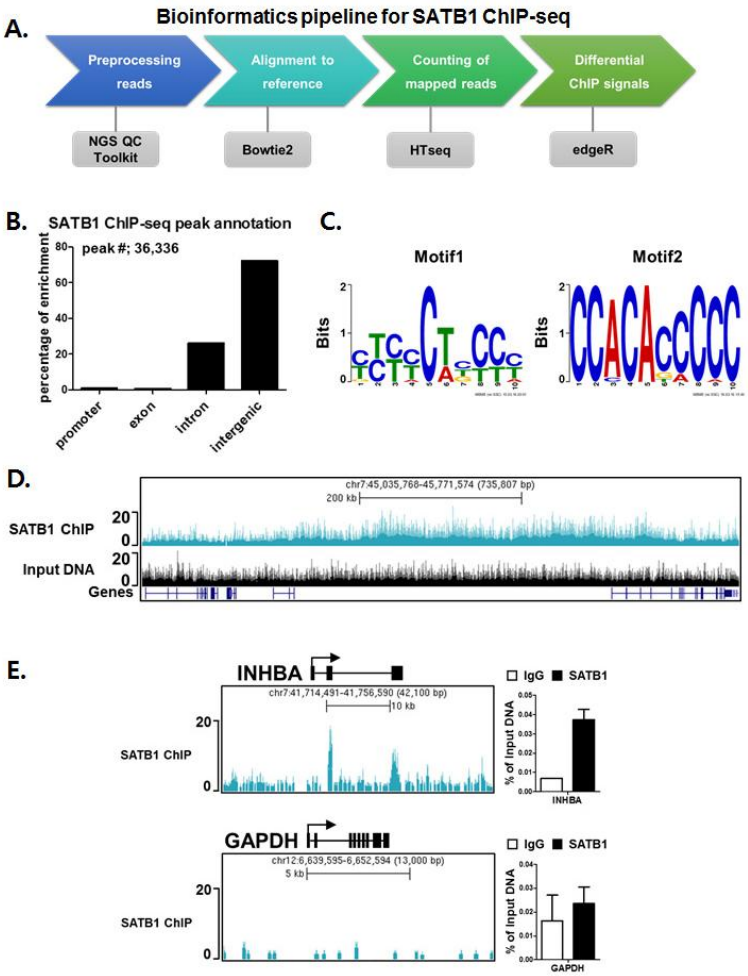

Figure 11. Distribution of SATB1 binding. A. Schematic representation of SATB1 ChIP-sequencing analysis workflow. B. The distribution of SATB1 binding was analyzed based on location including promoter, exon, intron and intergenic regions. C. The major consensus sequence feature for SATB1. D. A snapshot of the representative genome browser showing the SATB1 binding. E. Validation of SATB1 ChIP-seq data by real-time PCR analysis. Values represent mean S.D for technical duplicates from a representative experiment. All experiments were performed in triplets and the results were similar.

Table 9. Summary of SATB1 ChIP-seq mapping statistics

	Input DNA	SATB1 ChIP
Total number of reads	29,668,218	37,735,874
Total number of HQ reads	28,245,854	36,236,560
Unique mapped read number	11,781,762 (83.42%)	14,082,587 (77.73%)
Overall alignment rate	97.66%	96.07%
Average read length (base)	101	101

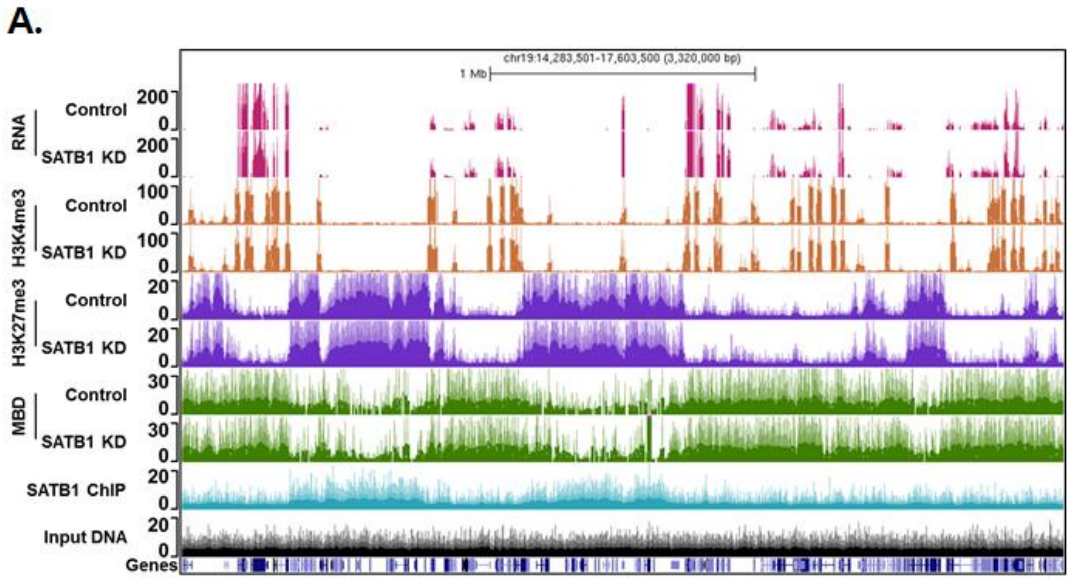

Figure 12. Integrated epigenomic profile. A. Generation of comprehensive epigenomic maps of transcriptome, histone modification, DNA methylome and SATB1 binding sites.

7. Integrated analysis of SATB1-dependent gene expression and epigenome in MDA-MB-231

When SATB1 regulates its target genes, SATB1 binds to the target gene loci and recruits histone modification enzymes.[29,30] To identify whether SATB1 simultaneously affects gene expression and histone modification or DNA methylation, we performed an integrated analysis of gene expression profiling and epigenomic profiling for histone active marker (H3K4me3), repressor marker (H3K27me3) or DNA methylation.

As a result, we found that 132 genes showed significant overlap in gene expression and H3K4me3 modification by SATB1 (Figure 13A-B). In addition, 228 genes including CXCL1 and MTRNR2L1 coincided with gene expression and H3K27me3 enrichment by SATB1 (Figure 14A-B). We also analyzed the correlation between transcription and DNA methylation by SATB1. When gene expression was changed by SATB1, 161 genes including POP5 and HLA-F was simultaneously affected by SATB1 (Figure 15A-B).

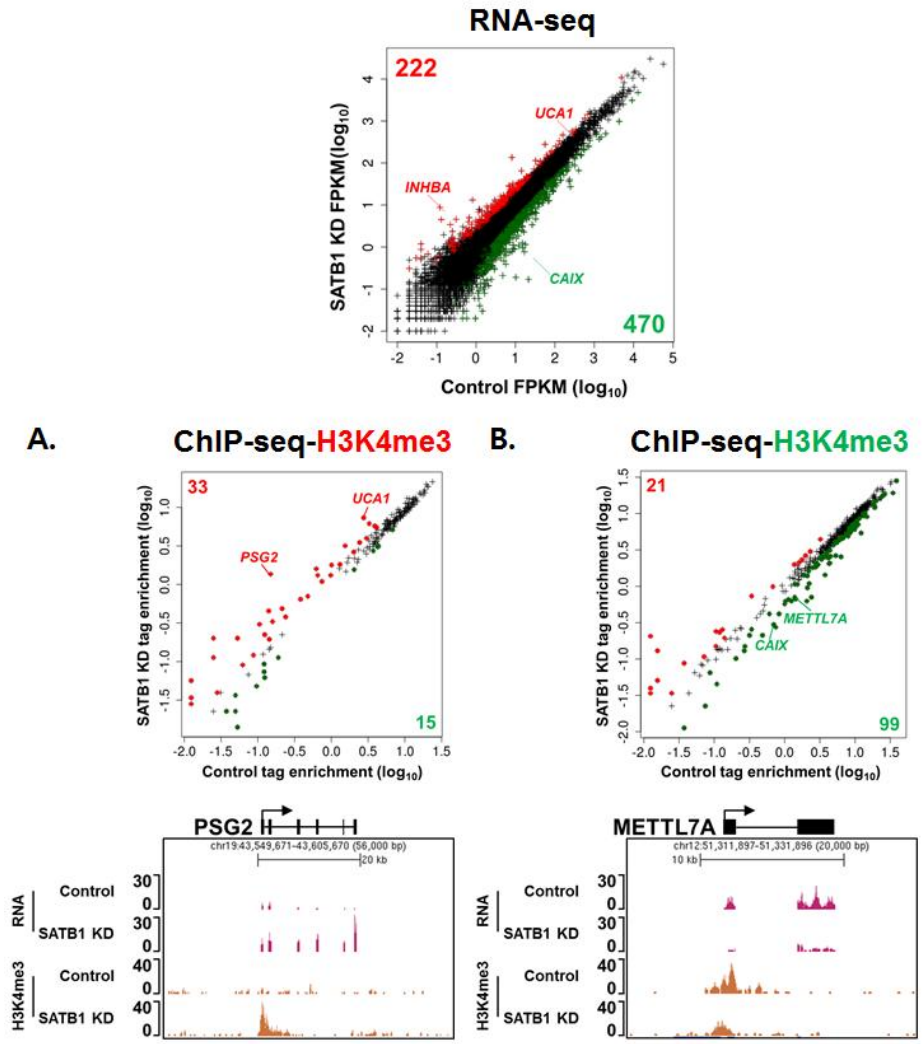

Figure 13. Epigenetically regulated SATB1 target genes that overlap RNA-seq and H3K4me3 ChIP-seq. A. 33 genes revealed transcript and enrichment of H3K4me3 which was downregulated by SATB1 (top panel). Snapshot of a representative gene is shown (bottom panel). B. 99 genes changed gene expression and presence of H3K4me3 was upregulated by SATB1 (top panel). METTL7A is shown as a representative gene (bottom panel).

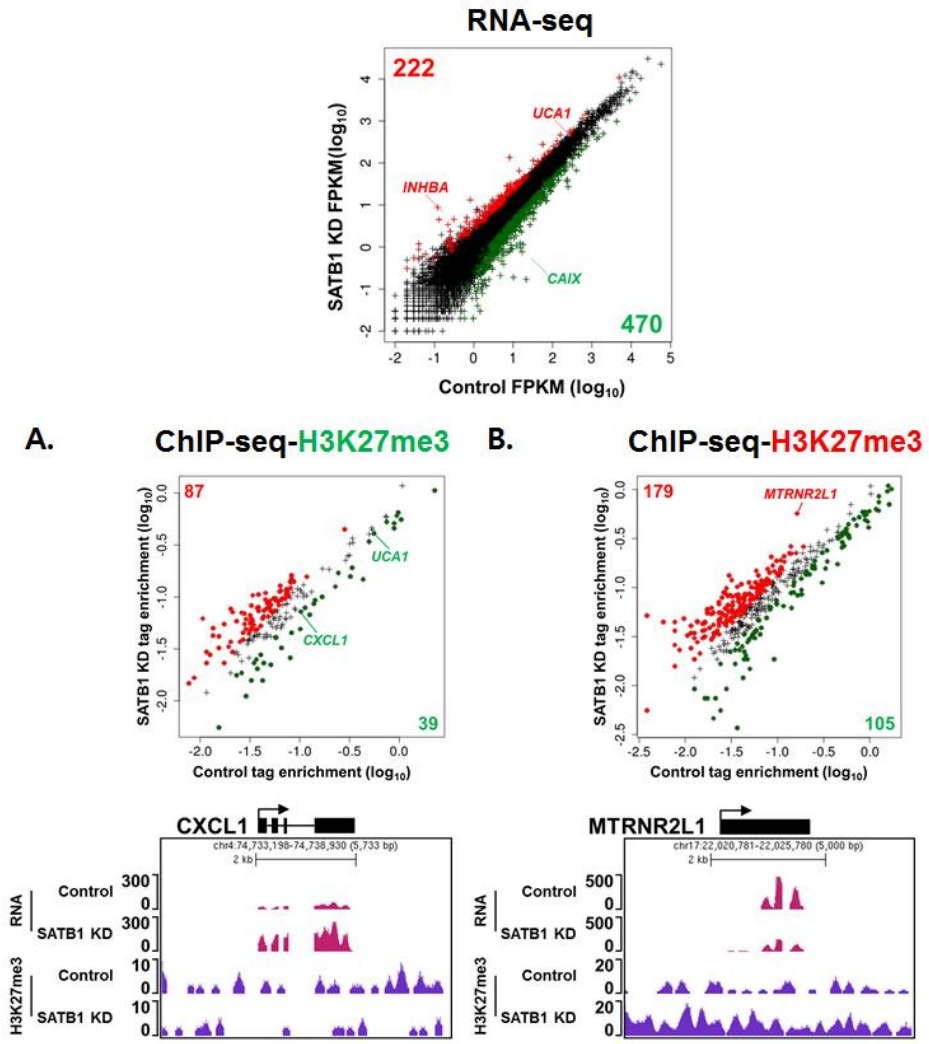

Figure 14. Epigenetically regulated SATB1 target genes that overlap RNA-seq and H3K27me3 ChIP-seq. A. 39 genes revealed transcript and enrichment of H3K27me3 was regulated by SATB1 (top panel). Snapshot of a representative gene is shown (bottom panel). B. 179 genes changed gene expression and presence of H3K27me3 was regulated by SATB1 (top panel). MTRNR2L1 is shown as a representative gene (bottom panel).

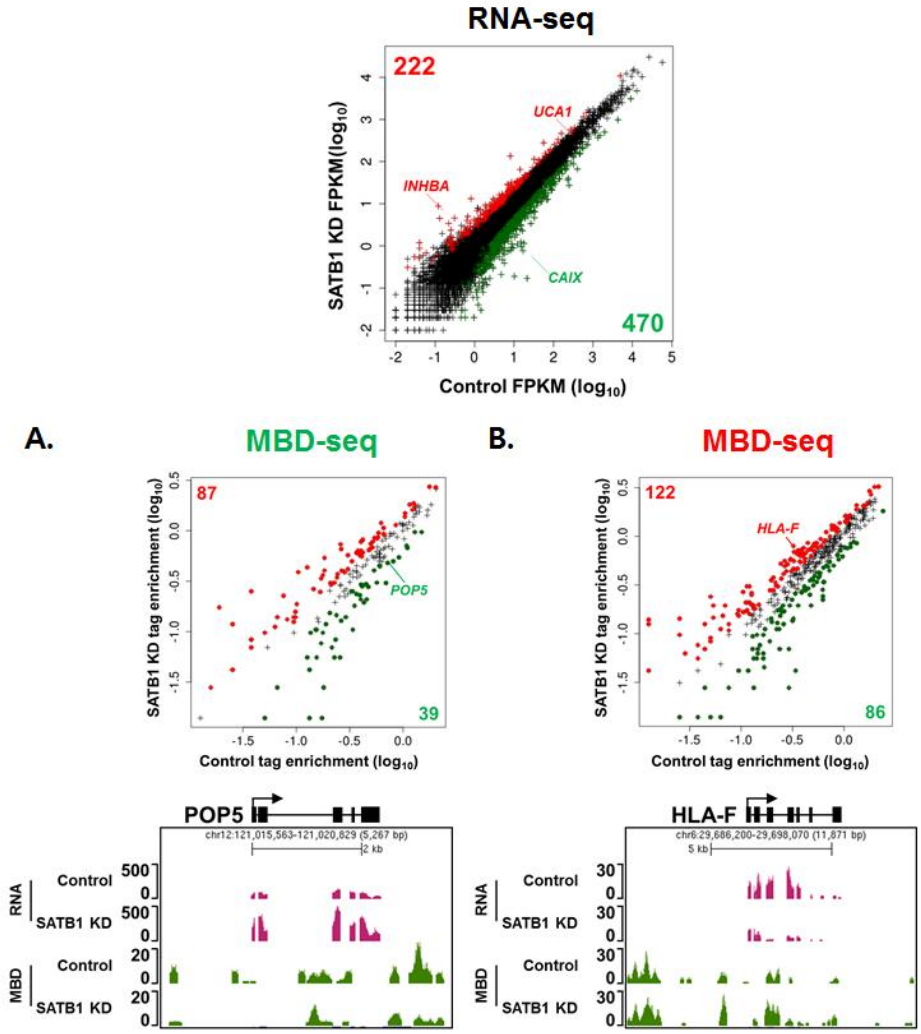

Figure 15. Epigenetically regulated SATB1 target genes that overlap RNA-seq and MBD-seq. A. 39 genes revealed transcript and status of DNA methylation was regulated by SATB1 (top panel). POP5 is shown as a representative gene (bottom panel). B. 122 genes changed gene expression and DNA methylation status which was regulated by SATB1 (top panel). HLA-F is shown as a representative gene (bottom panel).

8. SATB1 is required for efficient expression of CAIX

It has recently been reported that, carbonic anhydrase IX (CAIX), which is induced by hypoxia, regulates the pH of nearby cells, affecting various cancer and metastasis.[69-72] Also, investigation of tumor microenvironment has increased as well as genetic and epigenetic aspects of tumorigenicity.[73] Specifically, the relationship between CAIX and tumor microenvironment has been reported, with CAIX playing a critical role as a pH regulator.[74,75] However the precise mechanism as to how CAIX modulates pH is unclear. We hypothesized that SATB1 contributes to CAIX expression in metastatic breast cancer. To confirm our hypothesis, our result of RNA-seq and histone ChIP-seq was validated (Figure 16A). We confirmed that CAIX expression was upregulated by SATB1 through independent real-time PCR (Figure 16B). We demonstrated that SATB1 plays an important role in CAIX expression through frequently binding H3K4me3 in the promoter region of CAIX, but did not relate binding H3K27me3 (Figure 16B). Furthermore, to determine whether other histone modification markers and corepressor maker regulates CAIX expression, ChIP was performed for H3K4me1 and H3K27Ac, which are known enhancer markers, and Ezh2, which is related to the regulation of H3K27me3 (Figure 16B). These data indicated CAIX expression is significantly affected by H3K4me3, H3K4me1 and H3K27Ac whereas H3K27me3 and Ezh2 did not affect CAIX expression.

To identify whether SATB1 directly regulates CAIX expression, we performed ChIP coupled with real-time PCR and luciferase assay. SATB1 bound 0.2 kb upstream from CAIX the transcription start sites (TSS) in depleted-SATB1 MDA-MB-231 cells (Figure 17A-B).

SATB1 affected CAIX promoter activity through loss-of function (Figure 17C). These data exhibit that SATB1 directly binds to CAIX promoter, stimulating CAIX expression. In addition, while previous study demonstrated that hypoxic condition induced CAIX expression, this was inhibited through the presence of SATB1 (Figure 17D). SATB1 also slightly repressed CAIX-induced extracellular acidification (Figure 17E).

As it has been previously reported that aberrant expression of CAIX promotes various cancer, we confirmed a correlation between CAIX and metastasis. To determine the role of CAIX in breast cancer cells, we performed depleted-CAIX using siRNA. CAIX mRNA level decreased in depleted of CAIX (Figure 18A). To determine whether SATB1 regulates CAIX expression upstream, CAIX and SATB1 mRNA expression were quantitated in depleted-CAIX and under normoxic or hypoxic condition. SATB1 expression was irrelevant to these condition (Figure 18A). Collectively, SATB1 may be a prerequisite for efficiently expressing CAIX. Furthermore, we evidenced whether CAIX modulated tumorigenesis through apoptosis and transwell cell migration and invasion assay. As a result, absence of CAIX induced cell apoptosis and prevented cell invasion and migration, indicated that CAIX promotes aggressive cancer behavior *in vitro* (Figure 18B-D).

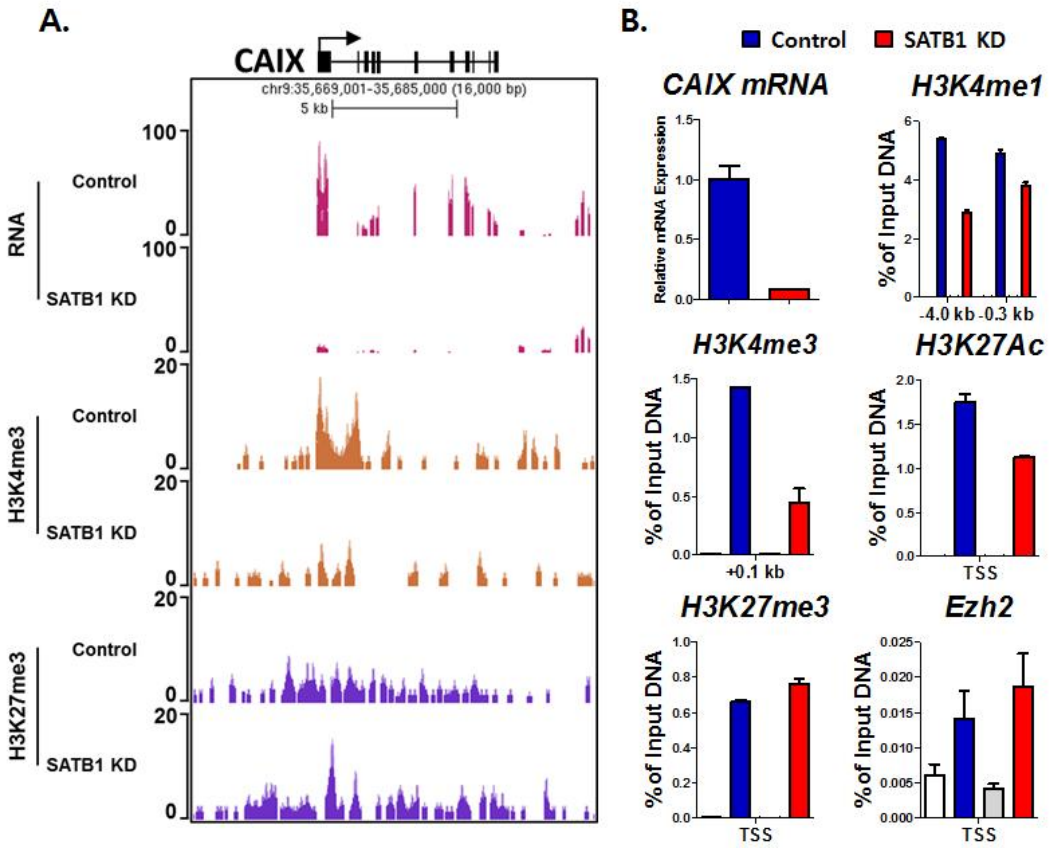

Figure 16. Epigenetic regulation of CAIX by SATB1. A. Visualization of CAIX locus for RNA-seq and ChIP-seq. B. Validation of CAIX mRNA, relative to GAPDH, were quantitated by real-time PCR. Validations of ChIP-seq for H3K4me3 or H3K27me data were quantitated by real-time PCR. In addition, ChIP for H3K4me1, H3K27Ac and Ezh2 were quantitated by real-rime PCR. Values represent mean S.D of technical duplicates from a representative experiment. All experiments were performed in triplets with similar results.

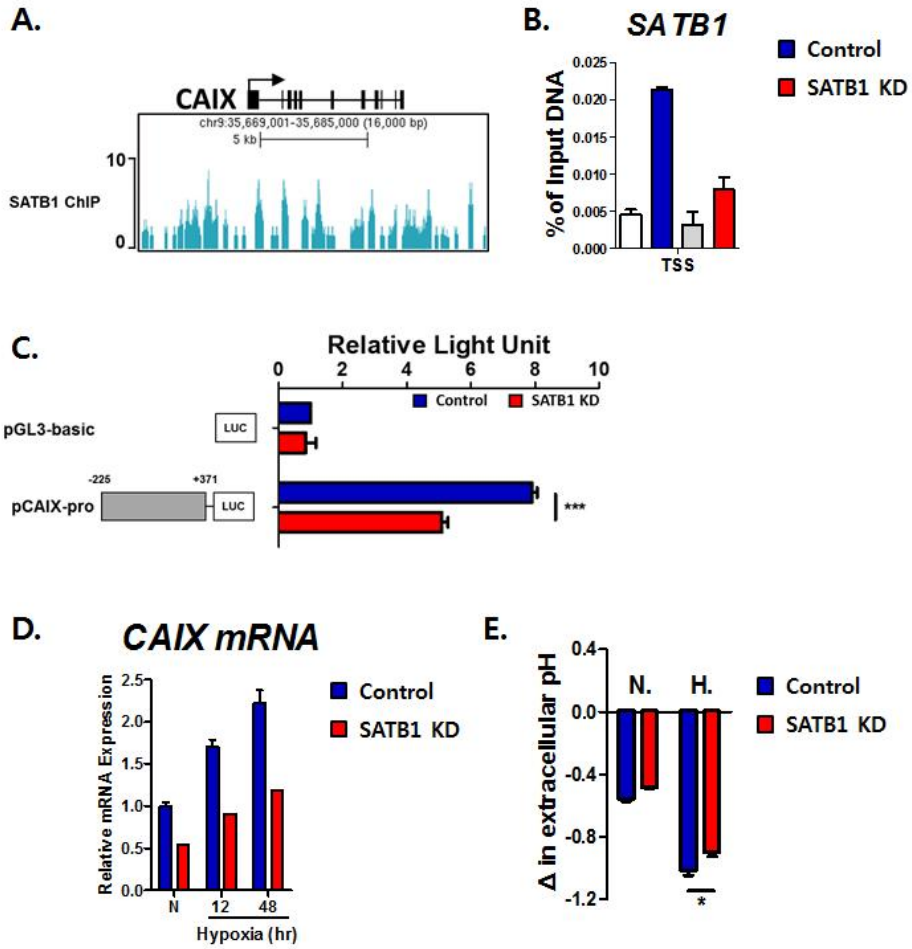

Figure 17. CAIX is the direct target gene of SATB1. A. Snapshot of CAIX locus genome browser shows the SATB1 reads in MDA-MB-231 cells. B. ChIP for SATB1 was quantitated by real-time PCR. C. luciferase reporter contains CAIX promoter were transfected into depleted-SATB1 MDA-MB-231 cells. D. CAIX mRNA, relative to GAPDH, was quantitated by real-time PCR under normoxia or hypoxia condition for 12 or 48 hr. E. Extracellular pH was changed by SATB1 in normoxia or hypoxia condition for 24 hr. For each sample, the bar indicates S.D from three experiments.

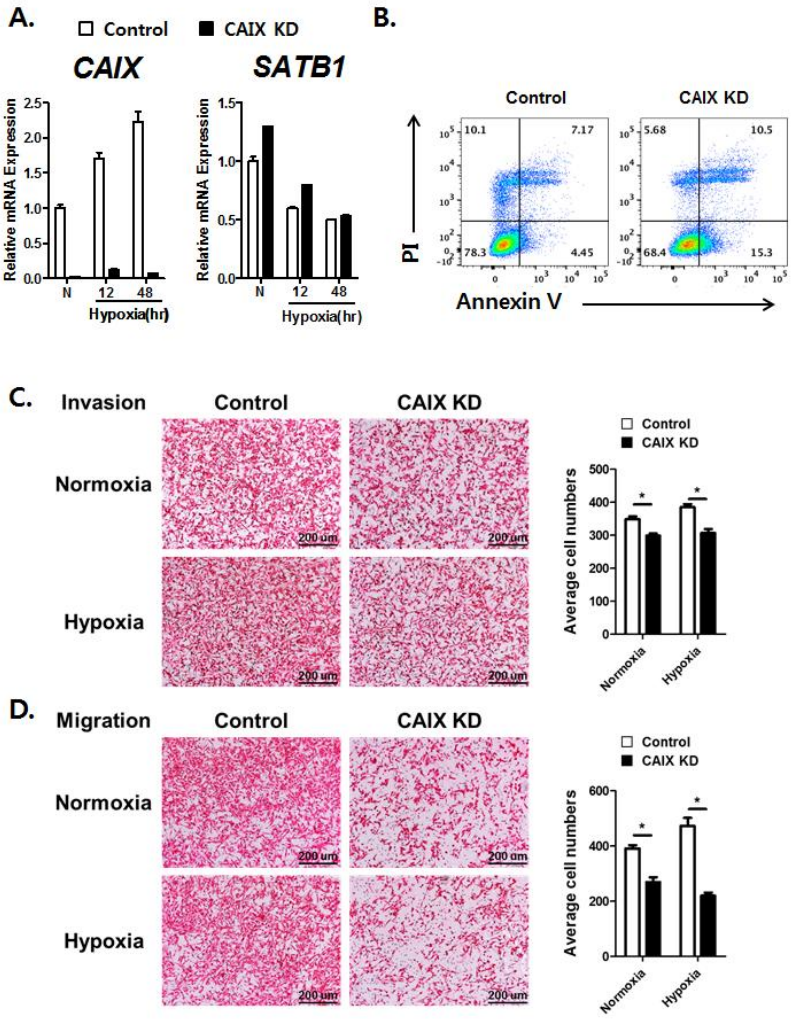

Figure 18. CAIX modulates tumor-associated cell migration and invasion. A. CAIX and SATB1 mRNA, relative to GAPDH, were quantitated by real-time PCR in depleted-CAIX MDA-MB-231 cells under normoxia or hypoxia condition for 12 or 48 hr. B. Flow cytometric analysis of apoptotic cells after transfection of siRNA-CAIX. C and D. Transwell invasion and migration assay of CAIX knockdown cells. For each sample, the bar indicates S.D from three experiments.

9. SATB1 is required for the repression of UCA1

We determined Urothelial cancer associated 1 (UCA1) as another target gene for SATB1. Recently, long noncoding RNAs (lncRNAs) arose as key regulator of metastasis and progression of tumorigenesis that interacts with DNA, RNA or Proteins.[76-78] During tumorigenesis, lncRNAs plays a critical role as an activator or a repressor. Among the lncRNA, UCA1 is associated to promote proliferation, motility, invasion and migration in various cancer. [79-84] Although, UCA1 expression is induced by SATB1 knockdown, we hypothesized that double knockdown of SATB1 and UCA1 would reverse cancer metastasis. This was validated through alteration of UCA1 expression and histone modification in UCA1 locus by SATB1 (Figure 19A). UCA1 mRNA was induced by shRNA-SATB1 independent experiment (Figure 19B). While histone active marker (H3K4me3) frequently bound to the UCA1 promoter, repressor marker (H3K27me) disrupted binding to the UCA1 promoter (Figure 19B). These data correlated with the result from RNA-seq and histone ChIP-seq. Next, we demonstrated whether the binding status of H3K27Ac and Ezh2 were dependent to SATB1. Histone acetylation status correlated with SATB1 and gene expression, whereas Ezh2 binding status was not related to SATB1 and gene expression (Figure 19B).

To identify whether SATB1 directly regulated UCA1 expression, we performed ChIP coupled with real-time PCR and luciferase assay. SATB1 actually bound 3.0 kb upstream and 0.8 kb downstream from the UCA1 transcription start sites (TSS) in the SATB1 knockdown cells (Figure 20A-B). The absence of SATB1 increased luciferase activity of

UCA1 promoter which contain the -3.0 kb regions (Figure 21C). These data exhibit that SATB1 directly binds to the UCA1 promoter promoting UCA1 expression.

Aberrant UCA1 expreesion has been reported to be associated withvarious cancers. Because we hypothesized that SATB1 and UCA1 has a synergic effect in tumorigenesis, we experimented with a double knockdown of SATB1 and UCA1 in MDA-MB-231 cells. To establish the shRNA system, we quantitated mRNA expression. While UCA1 showed increased expression by shRNA-SATB1, interestingly double knockdown resulted in an inhibition of UCA1 expression (Figure 21A). To determine, whether depletion of SATB1 and UCA1 affects cell growth, we performed cell apoptosis and cell proliferation. Knockdown of SATB1 and UCA1 led to extreme apoptosis and suppressed cell proliferation compared to when either SATB1 or UCA1 was absence in MDA-MB-231 cells, respectively (Figure 21B-C). However, we could not perform experiments to identify cell migration and invasion. These data suggest that synergic effects of SATB1 and UCA1 induced metastasis and progression in breast cancer.

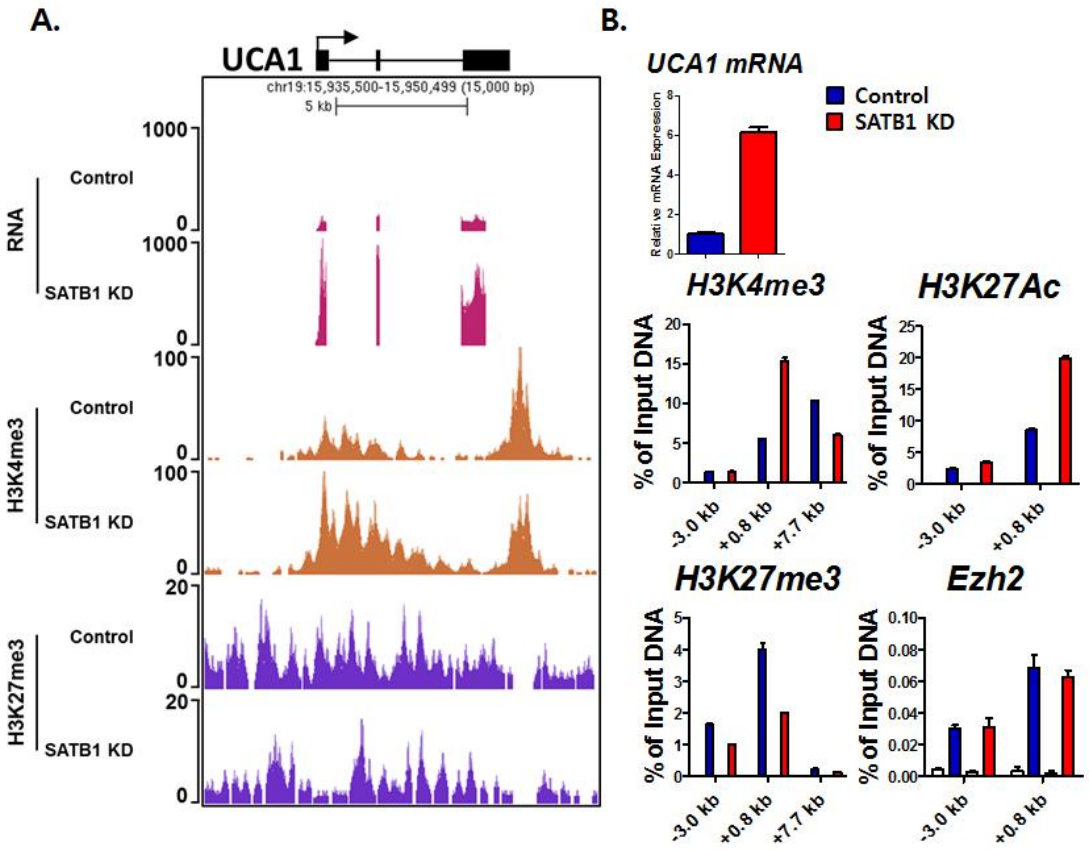

Figure 19. Epigenetic regulation of UCA1 by SATB1. A. Visualization of UCA1 locus for RNA-seq and ChIP-seq. B. Validation of UCA1 mRNA, relative to GAPDH, were quantitated by real-time PCR. Valdation of ChIP-seq for H3K4me3 or H3K27me data was quantitated by real-time PCR. ChIP for H3K27Ac and Ezh2 were quantitated by real-rime PCR. Values represent mean S.D of technical duplicates from a representative experiment. All experiments were performed in triplets showing similar results.

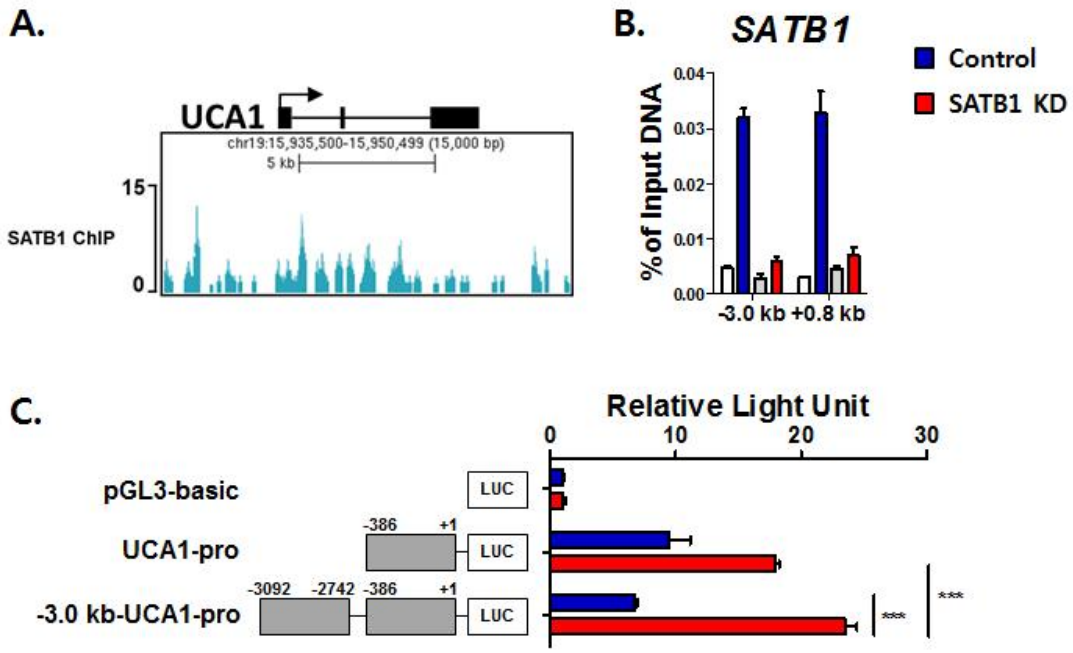

Figure 20. UCA1 is the direct target gene of SATB1. A. Snapshot of UCA1 locus genome browser shows the SATB1 reads in MDA-MB-231 cells. B. ChIP for SATB1 was quantitated using real-time PCR. C. luciferase reporter contains UCA1 promoter with or without -3.0 kb regions was transfected into depleted-SATB1 MDA-MB-231 cells. For each sample, the bar indicates S.D from three experiments.

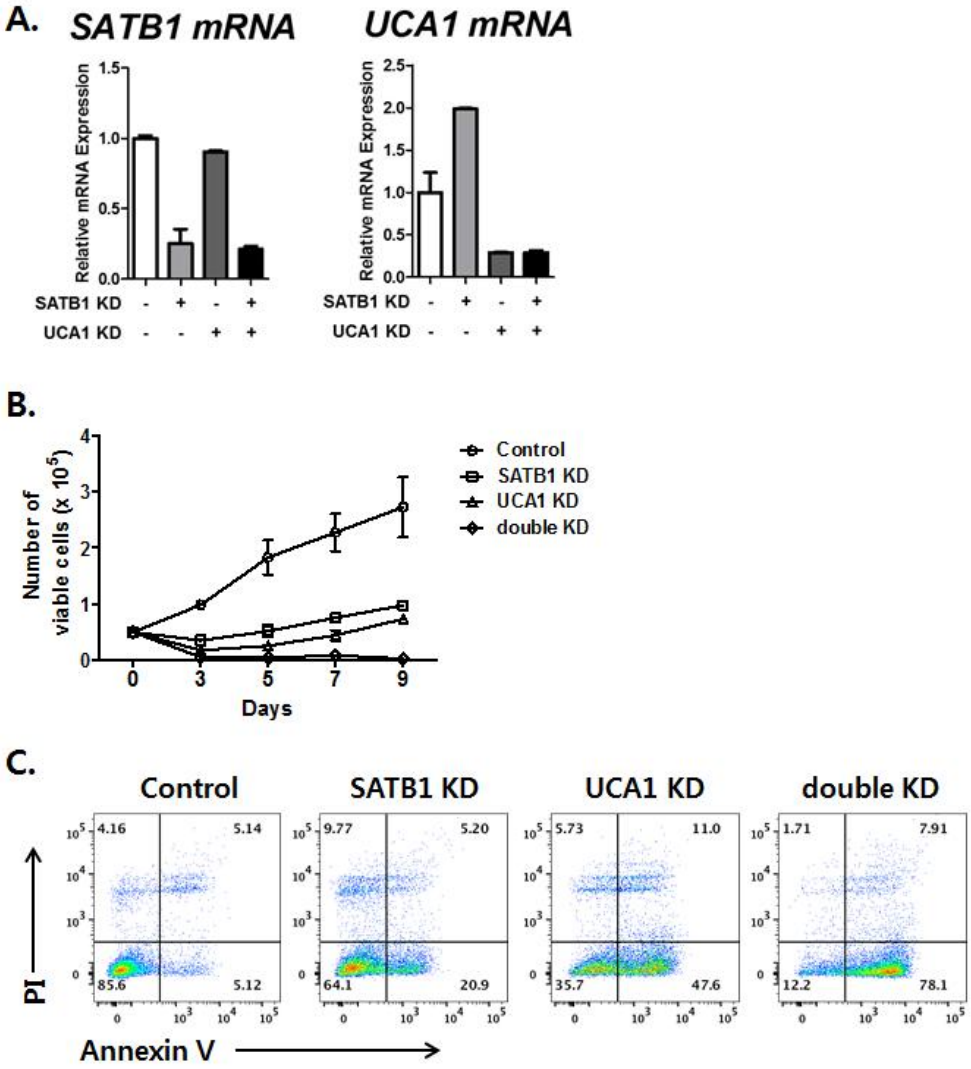

Figure 21. UCA1 regulates tumor growth and apoptosis. A. SATB1 and UCA1 mRNA, relative to GAPDH, were quantitated by real-time PCR in depleted-SATB1 or / and UCA1 MDA-MB-231 cells. B. Viability of cells was counted after trypan blue staining. C. Flow cytometric analysis of apoptotic cells induced by depleted-SATB1 and UCA1. For each sample, the bar indicates S.D from three experiments.

IV. DISCUSSION

In this study, we propose new biomarkers though transcriptome and epigenome which is regulated by SATB1. The previous studies defined that SATB1 is able to promote tumor progression and metastasis by globally remodeling the chromatin structure and regulating transcription. However these studies were performed using low-depth sequencing which has several limitations in genome-wide studies. To understand the highly quantitative and qualitative epigenetic mechanism of SATB1 targeted genes, we performed next-generation sequencing platform.

Breast cancer cell lines were selected before genome-wide studies were performed. This study shows SATB1 mRNA and protein level in various breast cancer cell lines. MDA-MB-231 cells were highly expressed than other breast cancer cell lines. We then established SATB1 lose-of function system in MDA-MB-231 cells. Through lenti-based shRNA systems, this study focused on gene expression and epigenetic mechanism according to the presence or absence of SATB1.

SATB1 regulation induced a poor prognosis phenotype that promotes tumor progression and metastasis similar to previous investigations. Additionally, SATB1 altered a large number of genes in breast cancer cells. We found that SATB1 evidenced the epigenetic profiles of SATB1-dependent genes though histone modification and DNA methylation. Our comprehensive integrated results of gene expression and histone modification analysis support the emerging links between chromatin remodeling factor, epigenetics and cancer.[85,86] Previous studies suggested that SATB1 modulates gene expression globally as, SATB1

tethers hundreds of gene loci onto its regulatory network and recruits chromatin modifying and transcription factors. The study of mechanistic cross-talk between histone modification and histone modifying enzymes is raised. However in this study, we did not explained about these point. Further study should be performed to explore the mechanism between SATB1 and histone modifying enzymes such as histone methyltrasferase and histone demethylases.

When SATB1 tethers chromatin loops into distinct domains, SATB1 recognizes matrix attachment regions which consists of ATC sequence.[20,87] However, due to the lack of SATB1 antibody, the precise mechanism as to how SATB1 binds to DNA sequence with specificity remains poorly understood. In this study, we primarily identified SATB1 binding sites at a genome-wide level.

Through comprehensive integrated RNA-seq data and ChIP-seq data of histone modifications, we found a large number of epigenetically regulated SATB1-depentent genes. Among the various candidates, our results suggest CAIX and UCA1 as epigenetic markers. We analyzed regulation mechanism of SATB1 target genes and tested their use as a diagnosis for the metastatic breast cancer. CAIX, as a pH regulator, induces extracellular acidification, facilitating tumor cell invasiveness. Interestingly, our results demonstrated that CAIX participates in the generation of an increasingly acidic extracellular space under hypoxia condition, on the other hand, SATB1 strongly block these processes. Future studies should be performed to explain how applicable this concept is in a 3D culture condition.

Although previous studies reported that UCA1 plays an oncogenic role in tumor growth and metastasis, our results shows that SATB1 negatively regulates UCA1 expression. Long

noncoding RNA (lncRNA) including UCA1, can be classified into having two major roles where cellular localization is present. Our present study has several limitations, we did not point out the relationship between SATB1 and UCA1 localization. Future studies will be performed to explain how the role of SATB1 affects the mechanism of UCA1 localization. In conclusion, CAIX and UCA1 is epigenetically regulated by SATB1, and may be potential biomarkers or useful therapeutic targets for metastatic breast disease.

V. CONCLUSION

In summary, we found that SATB1, regulator and chromatin organizer, affected tumorigenesis in metastatic breast cancer. Gene profiling and epigenomic profiling were monitored at a genome-wide level. We defined the relationship between SATB1 and Histone methylation. We analyzed epigenetically regulated mechanisms of SATB1 target genes and their use as potential diagnosis for the metastatic breast cancer.

- Chromatin organizer protein SATB1 regulates genome-wide histone modification status in the breast cancer cells
- Genome-wide SATB1 binding sites are identified
- Epigenetically regulated SATB1-target genes are identified
- SATB1 is required to maintain the permissive chromatin structure in the CAIX gene, which modulates tumor-associated cell migration and invasion
- SATB1 plays a crucial role to retain the repressive chromatin structure in the UCA1 gene, which regulates tumor growth and apoptosis
- SATB1 reprograms chromatin structure to promote breast tumor growth and metastasis

REFERENCE

1. Weigelt B, Peterse JL, van 't Veer LJ. Breast cancer metastasis: markers and models. Nat Rev Cancer 2005;5:591-602.
2. Perou CM, Sorlie T, Eisen MB, van de Rijn M, Jeffrey SS, Rees CA, et al. Molecular portraits of human breast tumours. Nature 2000;406:747-52.
3. Holliday DL, Speirs V. Choosing the right cell line for breast cancer research. Breast Cancer Res 2011;13:215.
4. Yokota J. Tumor progression and metastasis. Carcinogenesis 2000;21:497-503.
5. Hanahan D, Weinberg RA. Hallmarks of cancer: the next generation. Cell 2011;144:646-74.
6. Vargo-Gogola T, Rosen JM. Modelling breast cancer: one size does not fit all. Nat Rev Cancer 2007;7:659-72.
7. Dworkin AM, Huang TH, Toland AE. Epigenetic alterations in the breast: Implications for breast cancer detection, prognosis and treatment. Semin Cancer Biol 2009;19:165-71.
8. Sharma S, Kelly TK, Jones PA. Epigenetics in cancer. Carcinogenesis 2010;31:27-36.
9. Burgess DJ. Epigenetics. Dissecting driving DNA methylations. Nat Rev Cancer 2012;12:448-9.
10. You JS, Jones PA. Cancer genetics and epigenetics: two sides of the same coin? Cancer Cell 2012;22:9-20.
11. Blanco MA, Kang Y. Signaling pathways in breast cancer metastasis - novel insights from functional genomics. Breast Cancer Res 2011;13:206.
12. Dickinson LA, Joh T, Kohwi Y, Kohwi-Shigematsu T. A tissue-specific MAR/SAR DNA-binding protein with unusual binding site recognition. Cell 1992;70:631-45.
13. Burute M, Gottimukkala K, Galande S. Chromatin organizer SATB1 is an important determinant of T-cell differentiation. Immunol Cell Biol 2012;90:852-9.

14. Wang Z, Yang X, Chu X, Zhang J, Zhou H, Shen Y, et al. The structural basis for the oligomerization of the N-terminal domain of SATB1. Nucleic Acids Res 2012;40:4193-202.
15. Kumar PP, Purbey PK, Ravi DS, Mitra D, Galande S. Displacement of SATB1-bound histone deacetylase 1 corepressor by the human immunodeficiency virus type 1 transactivator induces expression of interleukin-2 and its receptor in T cells. Mol Cell Biol 2005;25:1620-33.
16. Notani D, Gottimukkala KP, Jayani RS, Limaye AS, Damle MV, Mehta S, et al. Global regulator SATB1 recruits beta-catenin and regulates T(H)2 differentiation in Wnt-dependent manner. PLoS Biol 2010;8:e1000296.
17. Kumar PP, Bischof O, Purbey PK, Notani D, Urlaub H, Dejean A, et al. Functional interaction between PML and SATB1 regulates chromatin-loop architecture and transcription of the MHC class I locus. Nat Cell Biol 2007;9:45-56.
18. Pavan Kumar P, Purbey PK, Sinha CK, Notani D, Limaye A, Jayani RS, et al. Phosphorylation of SATB1, a global gene regulator, acts as a molecular switch regulating its transcriptional activity in vivo. Mol Cell 2006;22:231-43.
19. Purbey PK, Singh S, Notani D, Kumar PP, Limaye AS, Galande S. Acetylation-dependent interaction of SATB1 and CtBP1 mediates transcriptional repression by SATB1. Mol Cell Biol 2009;29:1321-37.
20. Purbey PK, Singh S, Kumar PP, Mehta S, Ganesh KN, Mitra D, et al. PDZ domain-mediated dimerization and homeodomain-directed specificity are required for high-affinity DNA binding by SATB1. Nucleic Acids Res 2008;36:2107-22.
21. Alvarez JD, Yasui DH, Niida H, Joh T, Loh DY, Kohwi-Shigematsu T. The MAR-binding protein SATB1 orchestrates temporal and spatial expression of multiple genes during T-cell development. Genes Dev 2000;14:521-35.
22. Yasui D, Miyano M, Cai S, Varga-Weisz P, Kohwi-Shigematsu T. SATB1 targets chromatin remodelling to regulate genes over long distances. Nature 2002;419:641-5.

23. Cai S, Han HJ, Kohwi-Shigematsu T. Tissue-specific nuclear architecture and gene expression regulated by SATB1. Nat Genet 2003;34:42-51.
24. Cai S, Lee CC, Kohwi-Shigematsu T. SATB1 packages densely looped, transcriptionally active chromatin for coordinated expression of cytokine genes. Nat Genet 2006;38:1278-88.
25. Ahlfors H, Limaye A, Elo LL, Tuomela S, Burute M, Gottimukkala KV, et al. SATB1 dictates expression of multiple genes including IL-5 involved in human T helper cell differentiation. Blood 2010;116:1443-53.
26. Beyer M, Thabet Y, Muller RU, Sadlon T, Classen S, Lahl K, et al. Repression of the genome organizer SATB1 in regulatory T cells is required for suppressive function and inhibition of effector differentiation. Nat Immunol 2011;12:898-907.
27. Kondo M, Tanaka Y, Kuwabara T, Naito T, Kohwi-Shigematsu T, Watanabe A. SATB1 Plays a Critical Role in Establishment of Immune Tolerance. J Immunol 2016;196:563-72.
28. Han HJ, Russo J, Kohwi Y, Kohwi-Shigematsu T. SATB1 reprogrammes gene expression to promote breast tumour growth and metastasis. Nature 2008;452:187-93.
29. Mir R, Pradhan SJ, Galande S. Chromatin organizer SATB1 as a novel molecular target for cancer therapy. Curr Drug Targets 2012;13:1603-15.
30. Kohwi-Shigematsu T, Poterlowicz K, Ordinario E, Han HJ, Botchkarev VA, Kohwi Y. Genome organizing function of SATB1 in tumor progression. Semin Cancer Biol 2013;23:72-9.
31. Han B, Luan L, Xu Z, Wu B. Expression and biological roles of SATB1 in human bladder cancer. Tumour Biol 2013;34:2943-9.
32. Wan F, Cheng C, Wang Z, Xiao X, Zeng H, Xing S, et al. SATB1 overexpression regulates the development and progression in bladder cancer through EMT. PLoS One 2015;10:e0117518.

33. Nodin B, Johannesson H, Wangefjord S, O'Connor DP, Lindquist KE, Uhlen M, et al. Molecular correlates and prognostic significance of SATB1 expression in colorectal cancer. Diagn Pathol 2012;7:115.
34. Meng WJ, Yan H, Li Y, Zhou ZG. SATB1 and colorectal cancer in Wnt/beta-catenin signaling: Is there a functional link? Med Hypotheses 2011;76:277-9.
35. Fang XF, Hou ZB, Dai XZ, Chen C, Ge J, Shen H, et al. Special AT-rich sequence-binding protein 1 promotes cell growth and metastasis in colorectal cancer. World J Gastroenterol 2013;19:2331-9.
36. Zhang Y, Tian X, Ji H, Guan X, Xu W, Dong B, et al. Expression of SATB1 promotes the growth and metastasis of colorectal cancer. PLoS One 2014;9:e100413.
37. Brocato J, Costa M. SATB1 and 2 in colorectal cancer. Carcinogenesis 2015;36:186-91.
38. Cheng C, Lu X, Wang G, Zheng L, Shu X, Zhu S, et al. Expression of SATB1 and heparanase in gastric cancer and its relationship to clinicopathologic features. APMIS 2010;118:855-63.
39. Sun F, Lu X, Li H, Peng Z, Wu K, Wang G, et al. Special AT-rich sequence binding protein 1 regulates the multidrug resistance and invasion of human gastric cancer cells. Oncol Lett 2012;4:156-62.
40. Tu W, Luo M, Wang Z, Yan W, Xia Y, Deng H, et al. Upregulation of SATB1 promotes tumor growth and metastasis in liver cancer. Liver Int 2012;32:1064-78.
41. Li G, Yang D, Li X, Zhong K, Liu X, Bi M, et al. [Expression of SATB1 in hepatocellular carcinoma cell lines with different invasive capacities]. Nan Fang Yi Ke Da Xue Xue Bao 2012;32:986-90, 94.
42. Peng ZK, Yang DH, Li XH, Huang Y, Zhang GQ, Zhong KB, et al. [Expression of special AT-rich sequence-binding protein 1 mRNA in hepatocellular carcinoma and its clinical significance]. Nan Fang Yi Ke Da Xue Xue Bao 2011;31:1207-11.

43. Xiang J, Zhou L, Li S, Xi X, Zhang J, Wang Y, et al. AT-rich sequence binding protein 1: Contribution to tumor progression and metastasis of human ovarian carcinoma. Oncol Lett 2012;3:865-70.
44. Nodin B, Hedner C, Uhlen M, Jirstrom K. Expression of the global regulator SATB1 is an independent factor of poor prognosis in high grade epithelial ovarian cancer. J Ovarian Res 2012;5:24.
45. Zhao XL, Wang P. [Expression of SATB1 and BRMS1 in ovarian serous adenocarcinoma and its relationship with clinieopathological features]. Sichuan Da Xue Xue Bao Yi Xue Ban 2011;42:82-5, 105.
46. Elebro J, Heby M, Gaber A, Nodin B, Jonsson L, Fristedt R, et al. Prognostic and treatment predictive significance of SATB1 and SATB2 expression in pancreatic and periampullary adenocarcinoma. J Transl Med 2014;12:289.
47. Chen Z, Li Z, Li W, Zong Y, Zhu Y, Miao Y, et al. SATB1 Promotes Pancreatic Cancer Growth and Invasion Depending on MYC Activation. Dig Dis Sci 2015;60:3304-17.
48. Mao L, Yang C, Wang J, Li W, Wen R, Chen J, et al. SATB1 is overexpressed in metastatic prostate cancer and promotes prostate cancer cell growth and invasion. J Transl Med 2013;11:111.
49. Shukla S, Sharma H, Abbas A, MacLennan GT, Fu P, Danielpour D, et al. Upregulation of SATB1 is associated with prostate cancer aggressiveness and disease progression. PLoS One 2013;8:e53527.
50. Mao LJ, Zhang J, Liu N, Fan L, Yang DR, Xue BX, et al. Oncolytic virus carrying shRNA targeting SATB1 inhibits prostate cancer growth and metastasis. Tumour Biol 2015;36:9073-81.
51. Zhou LY, Liu F, Tong J, Chen QQ, Zhang FW. [Expression of special AT-rich sequence-binding protein mRNA and its clinicopathological significance in non-small cell lung cancer]. Nan Fang Yi Ke Da Xue Xue Bao 2009;29:534-7.

52. Selinger CI, Cooper WA, Al-Sohaily S, Mladenova DN, Pangon L, Kennedy CW, et al. Loss of special AT-rich binding protein 1 expression is a marker of poor survival in lung cancer. J Thorac Oncol 2011;6:1179-89.
53. Huang B, Zhou H, Wang X, Liu Z. Silencing SATB1 with siRNA inhibits the proliferation and invasion of small cell lung cancer cells. Cancer Cell Int 2013;13:8.
54. Li QQ, Chen ZQ, Xu JD, Cao XX, Chen Q, Liu XP, et al. Overexpression and involvement of special AT-rich sequence binding protein 1 in multidrug resistance in human breast carcinoma cells. Cancer Sci 2010;101:80-6.
55. Patani N, Jiang W, Mansel R, Newbold R, Mokbel K. The mRNA expression of SATB1 and SATB2 in human breast cancer. Cancer Cell Int 2009;9:18.
56. McInnes N, Sadlon TJ, Brown CY, Pederson S, Beyer M, Schultze JL, et al. FOXP3 and FOXP3-regulated microRNAs suppress SATB1 in breast cancer cells. Oncogene 2012;31:1045-54.
57. Mir R, Pradhan SJ, Patil P, Mulherkar R, Galande S. Wnt/beta-catenin signaling regulated SATB1 promotes colorectal cancer tumorigenesis and progression. Oncogene 2015.
58. Chen Z, Li Z, Li W, Zong Y, Zhu Y, Miao Y, et al. SATB1 Promotes Pancreatic Cancer Growth and Invasion Depending on MYC Activation. Dig Dis Sci 2015.
59. Patel RK, Jain M. NGS QC Toolkit: a toolkit for quality control of next generation sequencing data. PLoS One 2012;7:e30619.
60. Li B, Dewey CN. RSEM: accurate transcript quantification from RNA-Seq data with or without a reference genome. BMC Bioinformatics 2011;12:323.
61. Leng N, Dawson JA, Thomson JA, Ruotti V, Rissman AI, Smits BM, et al. EBSeq: an empirical Bayes hierarchical model for inference in RNA-seq experiments. Bioinformatics 2013;29:1035-43.
62. Langmead B, Salzberg SL. Fast gapped-read alignment with Bowtie 2. Nat Methods 2012;9:357-9.

63. Kent WJ, Sugnet CW, Furey TS, Roskin KM, Pringle TH, Zahler AM, et al. The human genome browser at UCSC. Genome Res 2002;12:996-1006.
64. Anders S, Pyl PT, Huber W. HTSeq--a Python framework to work with high-throughput sequencing data. Bioinformatics 2015;31:166-9.
65. Robinson MD, McCarthy DJ, Smyth GK. edgeR: a Bioconductor package for differential expression analysis of digital gene expression data. Bioinformatics 2010;26:139-40.
66. Robinson MD, Oshlack A. A scaling normalization method for differential expression analysis of RNA-seq data. Genome Biol 2010;11:R25.
67. Subramanian A, Tamayo P, Mootha VK, Mukherjee S, Ebert BL, Gillette MA, et al. Gene set enrichment analysis: a knowledge-based approach for interpreting genome-wide expression profiles. Proc Natl Acad Sci U S A 2005;102:15545-50.
68. Christiansen JJ, Rajasekaran AK. Reassessing epithelial to mesenchymal transition as a prerequisite for carcinoma invasion and metastasis. Cancer Res 2006;66:8319-26.
69. Li Y, Wang H, Oosterwijk E, Tu C, Shiverick KT, Silverman DN, et al. Expression and activity of carbonic anhydrase IX is associated with metabolic dysfunction in MDA-MB-231 breast cancer cells. Cancer Invest 2009;27:613-23.
70. Chen CL, Chu JS, Su WC, Huang SC, Lee WY. Hypoxia and metabolic phenotypes during breast carcinogenesis: expression of HIF-1alpha, GLUT1, and CAIX. Virchows Arch 2010;457:53-61.
71. Li Y, Tu C, Wang H, Silverman DN, Frost SC. Catalysis and pH control by membrane-associated carbonic anhydrase IX in MDA-MB-231 breast cancer cells. J Biol Chem 2011;286:15789-96.
72. Ivanova L, Zandberga E, Silina K, Kalnina Z, Abols A, Endzelins E, et al. Prognostic relevance of carbonic anhydrase IX expression is distinct in various

subtypes of breast cancer and its silencing suppresses self-renewal capacity of breast cancer cells. Cancer Chemother Pharmacol 2015;75:235-46.

73. Chadwick AL, Howell A, Sotgia F, Lisanti MP. Carbonic anhydrase 9 (CA9) and redox signaling in cancer-associated fibroblasts: therapeutic implications. Cell Cycle 2013;12:2534-5.
74. Gieling RG, Williams KJ. Carbonic anhydrase IX as a target for metastatic disease. Bioorg Med Chem 2013;21:1470-6.
75. Benej M, Pastorekova S, Pastorek J. Carbonic anhydrase IX: regulation and role in cancer. Subcell Biochem 2014;75:199-219.
76. Wang KC, Chang HY. Molecular mechanisms of long noncoding RNAs. Mol Cell 2011;43:904-14.
77. Klattenhoff CA, Scheuermann JC, Surface LE, Bradley RK, Fields PA, Steinhauser ML, et al. Braveheart, a long noncoding RNA required for cardiovascular lineage commitment. Cell 2013;152:570-83.
78. Mercer TR, Mattick JS. Structure and function of long noncoding RNAs in epigenetic regulation. Nat Struct Mol Biol 2013;20:300-7.
79. Wang XS, Zhang Z, Wang HC, Cai JL, Xu QW, Li MQ, et al. Rapid identification of UCA1 as a very sensitive and specific unique marker for human bladder carcinoma. Clin Cancer Res 2006;12:4851-8.
80. Shi X, Sun M, Liu H, Yao Y, Song Y. Long non-coding RNAs: a new frontier in the study of human diseases. Cancer Lett 2013;339:159-66.
81. Hiemer SE, Szymaniak AD, Varelas X. The transcriptional regulators TAZ and YAP direct transforming growth factor beta-induced tumorigenic phenotypes in breast cancer cells. J Biol Chem 2014;289:13461-74.
82. Huang J, Zhou N, Watabe K, Lu Z, Wu F, Xu M, et al. Long non-coding RNA UCA1 promotes breast tumor growth by suppression of p27 (Kip1). Cell Death Dis 2014;5:e1008.

83. Tian Y, Zhang X, Hao Y, Fang Z, He Y. Potential roles of abnormally expressed long noncoding RNA UCA1 and Malat-1 in metastasis of melanoma. Melanoma Res 2014;24:335-41.

84. Tuo YL, Li XM, Luo J. Long noncoding RNA UCA1 modulates breast cancer cell growth and apoptosis through decreasing tumor suppressive miR-143. Eur Rev Med Pharmacol Sci 2015;19:3403-11.

85. Baylin SB, Ohm JE. Epigenetic gene silencing in cancer - a mechanism for early oncogenic pathway addiction? Nat Rev Cancer 2006;6:107-16.

86. Drobic B, Dunn KL, Espino PS, Davie JR. Abnormalities of chromatin in tumor cells. EXS 2006:25-47.

87. Wang Z, Yang X, Guo S, Yang Y, Su XC, Shen Y, et al. Crystal structure of the ubiquitin-like domain-CUT repeat-like tandem of special AT-rich sequence binding protein 1 (SATB1) reveals a coordinating DNA-binding mechanism. J Biol Chem 2014;289:27376-85.

ABSTRACT (in Korean)

크로마틴 조절 인자인 SATB1 유전자에 의한 암 성장과 전이에 대한 후성유전학적 조절

< 지도교수 김 형 표 >

연세대학교 대학원 의과학과

이 종 주

Special AT-rich sequence binding protein 1 (SATB1)은 핵 안에 존재하여 크로마틴 구조를 변화 시키는 유전자로써, 이런 크로마틴 구조의 변화에 의해서 다양한 유전자 발현을 조절한다고 알려져 있다. 최초의 SATB1 유전자는 thymus 에서 발견되었고, 이로 인해 대부분의 SATB1 관련된 연구는 주로 T 세포에 관련해서 T 세포 발달과 분화에 대한 연구가 활발히 이루어졌다. 최근 유방암세포에서 SATB1 과 전이에 관한 보고가 발표된 이후 SATB1 에 대한 암에 관련된 연구가 증가하였다. SATB1 유전자는 유방암뿐만 아니라 폐암을 제외한 대부분의 암에서 과발현한다고 알려져 있으며, 이런 비정상적인 SATB1 유전자의

발현이 암전이 및 성장에 관련이 있다고 한다. SATB1 유전자가 암성장과 전이에 관련된 유전자 발현 크게 작용하지만, 이에 대한 조절기전, 특히 후성유전학적인 조절기전에 대한 연구는 미흡한 상태이다. 그래서 우리는 이번 연구를 통해서 SATB1 유전자에 의한 유전자 발현의 변화와 후성유전학적인 변화를 전유전체적인 차세대 염기서열을 분석하였다. 또한 SATB1 유전자의 결합부위를 전유전체적으로 분석함으로써 SATB1 유전자에 의한 발현조절의 직접적인 조절기전을 밝혔다. 이렇게 얻은 결과를 통합적으로 비교 분석하여 SATB1 유전자에 의해 발현이 변화하는 암성장과 전이에 관련된 새로운 바이오마커를 발굴 하고자 한다. SATB1 유전자의 의해 의존적으로 발현이 조절되는 타켓유전자가 전이성 유방암 바이오마커로서 기능하는지 탐색하기 위해 타겟유전자의 발현이 억제된 세포주를 대상으로 측정한 결과 암세포의 성장 및 전이 활성을 억제됨을 확인 할 수 있었다. 이 연구결과를 통해, SATB1 유전자에 의해 조절되는 후성유전학적 특성을 전유전체적으로 분석하였고 암성장과 전이에 영향을 주는 바이오마커를 발굴함으로써 앞으로 암을 효과적으로 진단하고 치유 할 수 있는 길이 열릴 것이다.

핵심되는말: 유방암, 후성유전학, SATB1, 크로마틴, 전유전체, 히스톤 변형, DNA 메틸화, 바이오마커

PUBLICATION LIST

1. Park JH, Choi Y, Song MJ, Park K, **Lee JJ**, Kim HP. 2016. Dynamic Long-Range Chromatin Interaction Controls Expression of IL-21 in CD4+ T Cells. J Immunol. 196(10):4378-89.

2. Kim TG, Kim M, **Lee JJ**, Kim SH, Je JH, Lee Y, Song MJ, Choi Y, Chung YW, Park CG, Cho JW, Lee MG, Lee YS, Kim HP. 2015. CCCTC-binding factor controls the homeostatic maintenance and migration of Langerhans cells. J Allergy Clin Immunol. 136(3):713-24.

3. Song MJ, **Lee JJ**, Nam YH, Kim TG, Chung YW, Kim M, Choi YE, Shin MH, Kim HP. Modulation of dendritic cell function by Trichomonas vaginalis-derived secretory products. 2015 Rep. 48(2):103-8.

4. Yang WJ, Song MJ, Park EY, **Lee JJ**, Park JH, Park K, Park JH, Kim HP. 2013. Transcription factors Sp1 and Sp3 regulate expression of human ABCG2 gene and chemoresistance phenotype. Mol Cells. 36(4):368-75.

5. Jang YJ, Park HR, Kim TH, Yang WJ, **Lee JJ**, Choi SY, Oh SB, Lee E, Park JH, Kim HP, Kim HS, Lee J, 2012. High dose bisphenol A impairs hippocampal neurogenesis in female mice across generations. Toxicology. 296, 73-82

6. Park K, Park JH, Yang WJ, **Lee JJ**, Song MJ, and Kim HP, 2012. Transcriptional activation of the IL31 gene by NFAT and STAT6. Journal of Leukocyte Biology. 91(2):245-57.

7. **Lee JJ**, Park K, Shin MH, Yang WJ, Song MJ, Park JH, Yong TS, Kim EK, and Kim HP, 2011. Accessible chromatin structure permits factors Sp1 and Sp3 to regulate human TGFBI gene expression. Biochemical and Biophysical Research Communications. 409(2):222-8.

8. Jin W*, **Lee JJ***, Kim MS, Son BH, Cho YK, and Kim HP, 2011. DNA methylation-dependent regulation of TrkA, TrkB, and TrkC genes in human hepatocellular carcinoma. Biochemical and Biophysical Research Communications. 406(1):89-95 (* equal contribution)